Int J Physiol Pathophysiol Pharmacol 2022;14(2):90-113
www.ijppp.org /ISSN:1944-8171/IJPPP0140995

Original Article

Improved Aitongxiao prescription (I-ATXP) induces apoptosis, cell cycle arrest and blocks exosomes release in hepatocellular carcinoma (HCC) cells

Ming-Bo Huang[1*], Zhao Gao[2*], Meng Xia[2], Xiaoqing Zhao[2], Xiaoyuan Fan[2], Shijie Lin[2], Lifeng Zhang[2], Li Huang[2], Ailing Wei[3], Hu Zhou[2], Jennifer Y Wu[4], William W Roth[1], Vincent C Bond[1], Jing Leng[2]

[1]Department of Microbiology, Biochemistry and Immunology, Morehouse School of Medicine, Atlanta, Georgia 30310, USA; [2]Guangxi Key Laboratory of Translational Medicine for Treating High-Incidence Infectious Diseases with Integrative Medicine, Guangxi University of Chinese Medicine, Nanning 530200, Guangxi, China; [3]The First Affiliated Hospital of Guangxi University of Chinese Medicine, Nanning 530023, Guangxi, China; [4]Columbia College, Columbia University, New York, NY 10027, USA. [*]Equal contributors.

Received December 6, 2021; Accepted February 13, 2022; Epub April 15, 2022; Published April 30, 2022

Abstract: Background: Hepatocellular carcinoma (HCC) is the second most common malignancy globally, after lung cancer, accounting for 85-90% of primary liver cancer. Hepatitis B virus (HBV) infection is considered the leading risk factor for HCC development in China. HCC is a highly malignant cancer whose metastasis is primarily influenced by the tumor microenvironment. The role of exosomes in cancer development has become the focus of much research due to the many newly described contents of exosomes, which may contribute to tumorigenesis. However, the possible role exosomes play in the interactions between HCC cells and their surrounding hepatic milieu is mainly unknown. We discovered an Improved Aitongxiao Prescription (I-ATXP): an 80% alcohol extract from a mix of 15 specific plant and animal compounds, which had been shown to have an anticancer effect through inducing apoptosis and cell cycle arrest and blocking exosomes release in HCC cells. However, the anticancer mechanism of I-ATXP on human liver carcinoma is still unclear. Objective: Due to its inhibitory effects on chemical carcinogenesis and inflammation, I-ATXP has been proposed as an effective agent for preventing or treating human liver carcinoma. In this study, we aimed to explore the effect of I-ATXP on proliferation, apoptosis, and cell cycles of different HCC cell lines. We investigated the impact of I-ATXP on exosomes' secretion derived from these HCC cells. Methods: The inhibitory effect of I-ATXP on proliferation and cytotoxicity of HepG2, SMMC7721, HKCL-C3 HCC cell lines, and MIHA immortalized hepatocyte cell line was assessed by CCK-8 assay. The cell cycle distribution and cell apoptosis were determined by flow cytometry using Annexin V-FITC/PI staining. The expression of Alix and CD63 of exosome marker proteins was detected by western blotting. The exosome protein concentration was measured by a fluorescent plate reader. The exosome-specific enzyme activity was measured by acetylcholinesterase (AchE) assay, and exosome morphological characteristics were identified by transmission electron microscopy (TEM). Results: I-ATXP inhibited the growth of HCC cells in a dose and time-dependent manner. Flow cytometry analysis showed that I-ATXP induced G0/G1 phase arrest and cell apoptosis. The I-ATX reduced HepG2, SMMC7721, and HKCI-C HCC cell lines exosomes release and low-dose I-ATXP significantly enhanced the growth inhibition induced by 5-Fu. Western blot analysis shows that after HCC cell lines were treated with various concentrations of I-ATXP (0.125-1 mg/ml) for 24 h, exosomes derived from three different HCC cells expressed exosome-specific proteins Alix and CD63. Compared with the untreated group, with the increment of the concentration of I-ATXP, the expression of exosome-specific proteins Alix and CD63 were reduced. These results suggest that I-ATXP can inhibit the release of exosomes with Alix and CD63 protein from HCC cells. Conclusions: I-ATXP is a traditional Chinese medicine that acts as an effective agent for preventing or treating human liver carcinoma. (i) I-ATXP can effectively inhibit cell proliferation of different HCC cells in a time and dose-dependent manner. Compared with 5-Fu, I-ATXP exhibited more selective proliferation inhibition in HCC cells, displaying traditional Chinese medicine advantages on tumor therapy and providing the experimental basis for I-ATXP clinical application. (ii) I-ATXP can induce apoptosis and cell cycle arrest in HCC cells. The CCK-8 assay results indicated that I-ATXP could inhibit HCC cell proliferation mediated by apoptosis and cell cycle arrest. (iii) I-ATXP can inhibit both the exosome releases and expression of CD63, and Alix derived from HCC cells, but the exosomes derived from liver cancer cells affect liver cancer cells' biological properties such as proliferation, invasion, and migration. These suggest that I-ATXP may affect HCC cells via regulation of exosomes of HCC cells, further indicating the potential clinical values of I-ATXP for the prevention or treatment of human liver carcinoma.

Keywords: Improved-Aitongxiao prescription (I-ATXP), hepatocellular carcinoma (HCC) cell lines, cell cycle, apoptosis, exosomes, migration, invasion

Introduction

Primary liver cancer (HPC), including hepatocellular carcinoma (HCC), is one of the most common malignancies globally. Its fatality rate is second in the world, second only to lung cancer [54]. According to statistics, about 19.3 million cancer cases globally, roughly 905,677 patients had liver cancer [1, 54]. Liver cancer ranks as the leading cause of cancer-related deaths in Asian countries. It is the seventh most important contributor in the USA [1, 4, 5]. HCC accounts for 90% of primary liver cancers, with the remaining 10% mainly cholangiocarcinoma [6]. The incidence and mortality rates increase with age and are higher in men than women, and data showed that mortality due to HCC in the USA continues to rise [7]. Hepatitis B virus (HBV) infection is the primary risk factor for HCC development in China [1-3, 6, 8]. The most critical risk factor for HCC in the USA is hepatitis C infection, followed by hepatitis B infection, accounting for almost 75% of cases.

Various approaches have been taken for HCC therapies, including chemotherapy, partial hepatectomy, radiotherapy, cryo-ablation, liver transplantation, immunotherapy, and transcatheter arterial chemoembolization (TACE). Other systemic treatments, such as sorafenib (a vascular endothelial growth factor receptor and tyrosine kinase inhibitor), have been used in clinical settings to prolong survival in patients with advanced HCC. Lenvatinib, an oral multikinase inhibitor, showed better than the sorafenib in terms of overall survival, a higher objective response rate, and better progression-free survival in patients with HCC. Still, it needs a good liver function, which is critical in achieving therapeutic efficacy [55]. However, their therapeutic potential to date is limited due to the high cost and the significant side-effects associated with using these agents, such as toxicity and drug resistance [9, 10]. Therefore, exploring new strategies for the treatment of HCC is necessary.

There has been a growing interest in traditional herbal medicines as a promising source of more efficient anticancer drugs. Natural compounds for the prevention of initiation and progression of human cancers can be a valuable source for the chemoprevention of human cancer. Complementary and alternative medicine (CAM) is also one of the possible strategies for approaching HCC treatment. Traditional medicine derived from plants, animal parts, and minerals has been used for preventing and treating liver diseases in Asia for centuries [11-14]. And is now considered an essential component of the CAM system. In recent years, studies have highlighted traditional medicine's role in retarding HCC progression in combination with other treatment modalities. Traditional medicine has also been used for preventing HCC, either alone or in combination with other conventional therapies. More data have demonstrated that traditional medicine is an effective strategy to mitigate the financial and social burden associated with HCC [15]. However, a clear understanding of traditional medicine's role in HCC treatment and prevention requires further clinical research.

Exosomes are small endosome-derived vesicles, ranging from 30 and 100 nm in size; they are actively secreted from cells through the exocytosis pathway [15, 16]. Many types of cells produce exosomes, thought to be important in regulating the intercellular microenvironment via the delivery of biological molecules, such as proteins, RNA and DNA [17-19]. They also act as substance transport carriers for biological information exchange and in the genetic and epigenetic mechanisms of cells [20]. Not only do exosomes initiate downstream signals to target cells, but they also transfer genetic material to target cells [17]. Tumor cell-derived exosomes are involved in intercellular communication, tumor angiogenesis, tumor metastasis, and drug and radiotherapy resistance [21-23]. Specific proteins highly enriched in exosomes, such as Alix, Tsg101, Hsp70, CD9, CD63, and CD81, are commonly used as markers for exosome identification [24, 25]. Exosomes were shown to mediate the tumor cell microenvironment in order to promote cancer metastasis and progression [26-29]. Previous studies have shown that cancer cells release many exosomes and that the exosome components vary in different pathological and physiological conditions [30, 31]. The

contents of exosomes are precisely adjusted in tumor cells, which suggests that the exosomes may serve an essential role in the process of tumor formation and development [32]. In the pathogenesis of HCC, Yu et al. [33] found that the miRNA in exosomes has a significant regulatory effect, such as on the miR-17-92 molecular group, and that mainly miR-92a is overexpressed in HCC, indicating that it is related to the occurrence and development of malignant tumors. The expression level of miR-92a in exosomes may become a diagnostic marker for primary liver cancer.

Preliminary studies and clinical trials have found that the effective rate of Aitongxiao (ATX) in the treatment of patients with primary liver cancer with blood stasis and toxin syndrome is 88.89%, which can significantly reduce the AFP level of patients with primary liver cancer and improve the quality of life of patients [34]. Previous research has shown that ATX inhibited the proliferation and promoted apoptosis of human liver cancer cells SMMC-7721 and Bel-7404 [35]. The ATX could retain cells of liver cancer staying in G0/G1 phase and prevent the cells from the G1 phase to the S phase. It could also markedly improve apoptosis rates of cancer cells and induce apoptosis of liver cancer cells [36]. The data showed that it has growth inhibitory effects in liver cancer and detoxifies blood circulation.

Improved Aitongxiao prescription (I-ATXP) is a compound of 80% alcohol extracted from a mix of the combination of these 15 compounds. I-ATXP also significantly improves clinical manifestations such as liver pain, abdominal distension, loss of appetite, fatigue, tongue bleeding, and pulse astringency ascites and complications in early and mid-term liver cancer patients. It also improves the quality of life of patients by showing excellent anticancer efficacy prospects. Animal experimental studies have demonstrated that I-ATXP can inhibit mouse H22 hepatocellular carcinoma growth; the mechanism of inhibiting tumor growth may be related to down-regulating the expression of vascular endothelial growth factor (VEGF), p53, and p21 Ras gene and inducing apoptosis in hepatocellular carcinoma cells [37-39]. The Aitongxiao also improves survival in rats with transplanted hepatocellular carcinoma, and it inhibits cancer in rats with transplanted cancer. Its mechanism is probably related to deducing the cellular apoptosis in rats with transplanted liver cancer. The intensity of this effect is possible in direct ratio to the dosage of Aitongxiao [40]. The Aitongxiao granule has a regulative impact on miRNAs of replanted liver cancer rats. Its therapeutical effects relate to the miRNA's expression of liver cell cancer development [41]. However, the anticancer effect of I-ATXP on human liver carcinoma cells is still unclear.

This study demonstrated the anticancer effect of I-ATXP on HepG2, SMMC7721, and HKCl-C3 HCC cell lines. We identified that I-ATXP effectively inhibits the growth of three independent human liver cancer cell lines by inducing apoptosis and cell cycle phase G0/G1 arrest and blocking liver cancer cells-derived exosome release. Also, I-ATXP promoted the activation of caspase-3, upregulated p21 and p27 expression, and inhibited the activation of STAT3. Interestingly, liver cancer cell-derived exosomes induced TLR8 increase.

Materials and methods

Cell culture

The human liver hepatocellular carcinoma (HepG2) cells, SMMC7721 cells, HKCl-C3, and immortalized hepatocyte cell line (MIHA) were purchased from the American Type Culture Collection (ATCC, Manassas, VA, USA). HepG2, SMMC7721, HKCl-C3, and MIHA cells were routinely cultured in a humidified 5% CO_2 incubator (37°C) in RPMI1640 medium (Thermo Fisher Scientific, USA) supplemented with 10% fetal bovine serum (FBS), 100 U/ml penicillin, and 100 μg/ml streptomycin.

Reagents

An Annexin V-FITC/PI assay kit was purchased from BD Bioscience (Franklin Lakes, NJ, USA). The cell counting Kit-8 (CCK-8) was purchased from Shanghai Biyuntian Biotechnology Co., Ltd., while dimethyl sulfoxide (DMSO), 5-fluorouracil (5-Fu), penicillin, and streptomycin were obtained from Sigma-Aldrich (St. Louis, MO, USA). Fetal bovine serum (FBS) was purchased from Clark Bioscience (Seabrook, MD, USA). The ExoQuick-TC Exosome Precipitation Kit was purchased from System Biosciences Inc. (SBI, Mountain View, CA, USA), and miRCURY

Exosome Isolation Kit was purchased from EXIQON (Woburn, MA, USA).

Antibodies

The following antibodies were used: (i) rabbit polyclonal anti-CD63 antibody (Abcam, Inc., Cambridge, MA, USA); (ii) goat polyclonal anti-Alix antibody (Santa Cruz Biotechm, Dallas, TX, USA); (iii) mouse monoclonal anti-tubulin antibody (Sigma-Aldrich, Inc., St. Louis, MO); (iv) goat anti-rabbit IgG (H+L) labeled with horseradish peroxidase (HRP) antibody (Thermo Fisher Scientific, Inc., Rockford, IL); (v) HRP-coupled goat anti-mouse IgG antibody (Thermo Fisher Scientific).

I-ATXP combination

Improved Aitongxiao prescription (I-ATXP) is a group of 80% alcohol extracted from 15 plant and animal compounds. They were Hedyotis diffusa willd 15 g, curcumae rhizoma 10 g, scutellariae barbatae herba 15 g, trionycis carapax 10 g, testudinis carapax et plastrum 10 g, ostreae concha 10 g, auranth fructus 10 g, astragali radix 15 g, codonopsis radix 10 g, eucommiae cortex 10 g, sparganii rhizoma 10 g, peach kernel 10 g, paeoniae radix rubra 15 g, glycyrrhizae radix et rhizome 5 g, and onychiumjaponicum (Thunb) kunze var japonicum 20 g. Every pack I-ATXP (total combination) contains 250 g I-ATXP. The theory of traditional Chinese medicine behind the variety of these 15 compounds divided into four groups according to their role: (i) Sovereign compounds: Hedyotis diffusa willd, Scutellariae barbatae, and Kunze var. japonicum have Clearing heat, detoxifying and anti-tumor. (ii) Minister compounds: Auranth fructus, Sparganii rhizome, Curcumae rhizome, Peach Kernel, Paeoniae radix rubra, Trionycis carapax, Ostreae concha, which have dredging liver and regulating qi, promoting blood and removing stasis, eliminating stagnation and relieving pain. (iii) Assistant compounds: Astragali radix, Codonopsis redix, Testudinis carapaxet plastrum, Eucommiae cortex which have replenishing qi and nourishing blood, reinforcing liver and kidney. (iv) Guiding compound/courier compound: Glycyrrhizae radixet rhizome has moderated other herbal medicines. I-ATXP was purchased from the First Affiliated Hospital of the Guangxi University of Chinese Medicine. The I-ATXP was extracted with 80% ethanol and dissolved in DMSO. 5-FU (5-fluorouracil, 0.25 g/10 ml) was used as the control treatment and purchased from Shanghai Xudong Haipu Pharmaceutical Co., Ltd.

I-ATXP preparation and extraction

250 g of the drug mix was added to 80% ethanol and soaked overnight, heated in a water bath for 1.5 hours, and extracted three times. After the extract was filtered by suction, the filtrate was synthesized and concentrated under reduced pressure with a rotary evaporator and then evaporated to dryness in a water bath. Crude extract of Aitongxiao recipe reported by Jiang Lin et al. [42] showed that the extraction method of 80% alcohol has high active ingredients, few impurities, and an easy operation. Therefore, in this study, we followed the technique of crude compound extraction, and this was used for follow-up experiments. (a) we took the pack as the unit, crushed the medicine into powder according to the corresponding extraction method, put it into the corresponding solvent (250 g/pack, six-fold water, total 1500 ml solvent), and let it soak overnight; (b) we built the reaction equipment; (c) we heated the medicine using the reflux start time as the starting point for timing (when the condenser tube starts to drip), filtered for 1 hour each time, and collected the medicine once; (d) we used the rotary evaporator to recover alcohol; (e) we used a cloth funnel to filter the concentrated medicinal solution. When the water-extracted medicinal liquid has evaporated to a volume of ≥ 750 ml, we added 1285.7 ml of 95% alcohol to dilute the alcohol to a 60% concentration; (f) we evaporated, concentrated the medicine to a paste, and finally collected the ointment. The net weight of the cream extracted with 85% alcohol was 86.12 g. Because the total weight of the crude drug extracted with 85% alcohol was 750 g, the ratio of crude drug to pure ointment was 750:86.12, or equal to 8.7. The amount of crude drug contained in each gram of pure cream is 8.7 g. We set the concentration to 1 mg/ml and converted it to 8.7 mg/ml crude drug concentration.

Cell proliferation and cytotoxicity assay

Cell proliferation and cytotoxicity were examined by CCK-8 assay. CCK-8 allows sensitive

colorimetric assays for the determination of cell viability in cell proliferation and cytotoxicity assays using WST-8 (2-(2-methoxy-4-nitrophenyl)-3-(4-nitrophenyl)-5-(2,4-disulfophenyl)-2H-tetrazolium, monosodium salt), which produces a water-soluble formazan dye upon bio reduction in the presence of an electron carrier, 1-Methoxy PMS. CCK-8 solution was added directly to the cells; no pre-mixing of components as required. Dehydrogenase activities reduced WST-8 in cells to give a yellow-color formazan dye soluble in the tissue culture media. The amount of the formazan dye generated by dehydrogenases in cells was directly proportional to the number of living cells. In this study, cells were seeded into 96-well culture plates (5000 cells/well/100 μl) and incubated in 5% CO_2 at 37°C. After incubation overnight, the cells were exposed to various concentrations of I-ATXP at 0.125 mg/ml, 0.25 mg/ml, 0.5 mg/ml, and 1 mg/ml individually, and 0.05 mg/ml, 0.1 mg/ml and 0.2 mg/mL of 5-FU as positive controls. We incubated the plate for 24, 48, and 72 hours in the incubator. The plate was washed twice with 1× PBS. Then, 100 μl of medium with 10 μl of CCK-8 solution was added to each well of the plate. We were careful not to introduce bubbles to the wells since they interfere with the O.D. reading. The cells were incubated for another 1-4 hours at 37°C in the incubator. Finally, the plate was measured at an absorbance of 450 nm by a Microplate Reader (Bio-Rad, Hercules, CA, USA). All experiments were repeated at least three times.

Cell-cycle analysis by flow cytometry

5×10^5 cells/well HepG2, SMMC7721, and HKCI-C3 cells were seeded into the 6-cm petri dish with each well containing 3 ml medium. After 24 hours incubation, the cells were treated with various concentrations of I-ATXP, 0.125 mg/ml, 0.25 mg/ml, 0.5 mg/ml, and 1 mg/ml individually, and 0.2 mg/ml of 5-FU as the positive control for 24 hours. The cells were then collected and fixed with 75% cold ethanol (1 ml PBS and 3 ml absolute ethanol) at -20°C overnight. Afterward, the cells were incubated with 200 μl RNase A (1 mg/ml) and 500 μl propidium iodide (PI, 100 μg/ml) for 30 min at room temperature in the dark and analyzed using the FACScan flow cytometer (Becton Dickinson, Franklin Lakes, NJ, USA).

Apoptosis assay via PI-Annexin-V stain by flow cytometry

Identification of apoptosis by PI-Annexin-V staining HepG2, SMMC7721, and HKCI-C3 liver cancer cells were made in 6-cm Petri dishes 24 h before treatment. The cells were treated with different concentrations of I-ATXP: 0.125 mg/ml, 0.25 mg/ml, 0.5 mg/ml and 1 mg/ml individually, 0.2 mg/ml 5-Fu as the positive control and mock as negative control. They were then incubated for 24 h and were harvested by trypsinization with 0.1% trypsin. Then, cells were stained with 5 μl Annexin V-FITC and 5 μl propidium iodide (PI) (20 μg/ml) and were incubated for 15 min at the darkroom temperature. Then, the cells were incubated with 200 μl RNase A (1 mg/ml) for 30 min at room temperature in the dark. The apoptotic cells were detected using a FACScan flow cytometer (Becton Dickinson, Franklin Lakes, NJ, USA).

Cell scratch assay

The cell scratch assay to test the wound-healing rates of HepG2 and SMMC-7721 cells were made as follows: cells were seeded in a 6-well plate until the cells grew to 90-95% confluency. The scratch wound was generated on the surface of the plates with a 20 μl pipette tip. Several concentrations of exosomes (0, 10 and 20 μg/ml) were co-cultured with cells for 24 h. The scratch area was photographed by a microscope at 0 and 12 h. Using Image J software, the changes of wound healing rate of HepG2 and SMMC-7721 cells were analyzed.

Cell migration and invasion assays

The cell migration and invasion assays were carried out using 24-well transwell chambers with an 8 μm pore polycarbonate membrane insert. In the migration assays, the HepG2 and SMMC-7721 liver cancer cells were seeded into the upper chambers (without Matrigel) at a density of 1×10^5 cells/well with 200 μl RPMI 1640 medium supplemented without FBS with several concentrations of exosomes derived from liver cancer cells (0, 10 and 20 μg/ml) added to the upper chambers, and 600 μl 10% FBS-1640 added to the lower wells. The plate was incubated at 37°C for 24 h. Then, cells were fixed, stained, and photographed under microscopy. Migration or invasion efficiency was determined by calculation of transferred-

cells number from five fields randomly picked. Each experiment was performed in triplicate. In the invasion assay, the HepG2 and SMMC-7721 liver cancer cells were seeded into the upper chambers (with Matrigel) at a density of 1×10^5 cells/well with 200 μl RPMI 1640 medium supplemented without FBS containing different concentrations of exosomes derived from liver cancer cells (0, 10 and 20 μg/ml) added to the upper chambers, and 600 μl 10% FBS-1640 added to the lower wells. The plate was incubated at 37°C for 24 h. After incubation for 24 h, the wells were collected. We performed cell fixation and staining, selecting 5 randomly under the microscope. Pictures of each field of view were taken for cell count. The invasion assay was performed in the same way as the migration assay above, except that the membrane was coated with Matrigel. An Olympus light microscope acquired the total number of cells invading and adhering to the lower surface (Olympus, Tokyo, Japan).

Exosome isolation and purification

The isolation of exosomes mainly involves six methods, which include differential ultracentrifugation [43, 44], polyethylene glycol (PEG) precipitation [45, 46], sucrose and iodixanol density ultracentrifugation [47], immunoaffinity (IAC) capture [48], size exclusion chromatography [49, 50] and qEV size exclusion column [51]. (i) Exosome isolation and purification for treatment: Exosomes were isolated from HepG2, SMMC7721, and HKCI-C3 liver cancer cells by the ExoQuick-TC Exosome Precipitation Kit (System Biosciencences [SBI], Mountain View, CA) and the manufacturer's instructions to isolate exosomes were followed. As a control, we used untreated tumor cells. Briefly, 10 ml of cell supernatants treated and untreated were centrifuged at 3000× g for 15 minutes. We transferred the 10 ml of supernatants to a clear tube, added 2 ml of ExoQuick-TC buffer, mixed well, and then incubated it at 4°C overnight. After incubation, the samples were centrifuged at 1500× g for 30 minutes. The pellets were centrifuged at 1500× g for 5 minutes. Finally, the exosome pellets were re-suspended with PBS and stored at 4°C or -80°C until used for analysis. (ii) Exosome isolation and purification for TEM by qEV size exclusion column. (a) Cell supernatants were centrifuged at 1500 rpm at 4°C for 5 min to remove cellular debris, and then the supernatants were centrifuged in 2000× g for 10 min at 4°C. Finally, the supernatants were centrifuged at 10,000× g for 30 min at 4°C, and we saved this supernatant. (b) We filtered the collected supernatant with a 0.22 μm filter membrane. (c) Initial concentration by ultrafiltration: we added 12 mL of the pretreated cell supernatant each time to a 15 ml, 100 kDa ultrafiltration tube and centrifuged horizontally at 5000× g at 4°C for 8 min. We discarded the supernatant of the outer tube, added an equal volume of the supernatant to be concentrated into the inner tube, and continued to centrifuge at 5000× g at 4°C. The centrifugation time was 2 min longer than the last centrifugation time. We repeated this step until there was only 4 ml of supernatant left in the inner tube of the ultrafiltration tube. We took it out and placed it in a 15 ml centrifuge tube. The inner wall of the ultrafiltration tube was then rinsed twice with PBS buffer, 2 mL each time. We transferred the liquid used to clean the inner tube wall of the ultrafiltration tube to a centrifuge tube containing 4 ml of supernatant to mix evenly. (d) Concentration by ultrafiltration again: we added 4 mL of supernatant each time to a 5 ml, 100 kDa ultrafiltration tube and centrifuged horizontally at 5000 g at 4°C for 8 min. We discarded the supernatant of the outer tube, added an equal volume of the supernatant to be concentrated into the inner tube, and continued to centrifuge at 5000× g at 4°C. The centrifugation time was 2 min longer than the last centrifugation time. We repeated this step until there was only 1 ml of supernatant left in the inner tube of the ultrafiltration tube. We then took it out and placed it in a 15 ml centrifuge tube. We rinsed the inner wall of the ultrafiltration tube with 1.5 ml of PBS buffer once and transferred it to a centrifuge tube containing 1 ml of supernatant to mix evenly. (e) QEV size exclusion column: we carefully removed the top cover and fixed the separation column vertically on the bracket for use. We removed the bottom cap, allowed 2 ml of buffer to flow down the separation column, and rinsed the separation column with 10 ml of PBS buffer. When all the buffers entered the sieve plate of the separation column, we added 500 μl of sample to the sieve plate through a pipette. We were careful not to drip onto the tube wall. The sample flowed into the separation column under the action of gravity. When the sample completely entered the sieve plate,

we added 2.5 ml PBS buffer solution. When the buffer solution completely entered the sieve plate, we added 1.5 ml PBS buffer solution and at the same time collected 1.5 ml liquid flowing down from the separation column. The liquid, which contains exosomes, was then collected. (f) We added 1.5 ml of exosome suspension to a 1.5 ml, 100 kDa ultrafiltration tube and centrifuged at 12,000 rpm at 4°C for 3 min. We discarded the supernatant of the outer tube, added an equal volume of the exosome suspension to be concentrated into the inner tube, and continued centrifugation at 12,000 rpm and 4°C. The centrifugation time was 2 min longer than the previous centrifugation time. We repeated this step until there was only 200 µl of exosome suspension left in the inner tube of the ultrafiltration tube. We took it out and placed it in a 1.5 ml EP tube. After aliquoting, we transferred it to -80°C for later use.

Transmission electron microscope (TEM)

Exosome morphological characteristics were identified by transmission electron microscopy (TEM). Briefly, the sample preparation process was as follows: we diluted the obtained exosomes (with a concentration of 5×10^{11} particles/ml) in at least 3 concentration gradients, and the dilution ratios were 5-fold, 10-fold, and 20-fold, respectively. Before dying, we took out 1% uranyl acetate from the refrigerator at 4°C and returned it to room temperature. We took out the exosomes sample from the refrigerator at -80°C, dropped 10 µl on the carbon film copper mesh, and waited for 1 min at room temperature. We used filter paper to remove excess sample from the edge of the copper mesh. 3 drops of 50 µl dye solution were pipetted onto the parafilm. We floated the copper mesh on each drop of dye solution drop and left the copper mesh on the third drop of dye solution for 1 min and absorbed the remaining liquid with filter paper. We dried the copper mesh at room temperature and observed it by transmission electron microscope (Hitachi Model HT7700 120 kV Compact-Digital Biological TEM, Hitachi High-Technologies Corporation, Tokyo, Japan).

Exosomes characterization by acetylcholinesterase (AchE) assay

Purified exosomes were quantitated by measurement of AchE as previously described. Briefly, we prepared 100 mM dithibionitrobenzoic (DTNB) as a stock color indicator and prepared 28.9 mg/mL in PBS of acetylthiocholine iodide as a stock substrate. Substrate stock can be stored at -20°C for one month, and color indicator can be stored at 4°C for two weeks. A working solution was prepared by mixing 10 ml of PBS with 200 µl of the substrate and 500 µl of DTNB. 50 µl of each exosome sample was transferred to 96 well microtitre plates, and then a standard curve was prepared using AchE from 0.98 mU/ml to 2000 mU/ml. After 50 µl of standards were added into separate wells, 200 µl of the working solution was added to all wells.

Immunoblot analysis

Cell proteins were analyzed using Western blot analysis as described previously by Huang et al. [52]. The protein samples were separated by SDS-PAGE on 4-20% Tris-HCl Criterion precast gels (Bio-Rad) and transferred to the nitrocellulose membrane electrophoretically. The membrane was washed in Tris-buffered saline (TBS; Bio-Rad) for 5 min, blocked with 5% nonfat milk in TTBS (TBS with 0.1% Tween 20) for 1 hour by shaking at room temperature, and processed for immunoblotting using a specific primary antibody with shaking at 4°C overnight, followed by a secondary HRP-conjugated IgG (H+L) antibody. Protein bands were detected by using the Western blotting luminol reagent (Santa Cruz Biotechnology, Inc., Santa Cruz, CA), followed by exposure to an image microscope. In some experiments, a stripping reagent was used to strip the membrane (Pierce Biotechnology, Rockford, IL), and hybridization with different primary and secondary antibodies was performed. Densitometry analysis was performed using ImageJ software (National Institutes of Health, Bethesda, MD).

Statistical analysis

Data are expressed as the mean ± standard deviation (S.D.). A two-sample t-test assuming equal variances was used to compare the differences between controls and treated samples in each group. A value of $P \leq 0.05$ was statistically significant.

Results

The cytotoxic effect of I-ATXP on different hepatocellular carcinoma cells and normal liver cells

To determine the cytotoxicity of I-ATXP, we used the CCK-8 assay to assess the IC50 (semi-inhi-

Table 1. Cytotoxicity of I-ATXP (IC50, mg/ml) in different liver cancer cells

Time	HepG2	SMMC7721	HKCI-C3	MIHA
24 h	2.189±0.472*	2.519±1.101*	1.827±0.326**	5.079±0.317
48 h	0.751±0.011*	0.941±0.154	0.913±0.025	1.151±0.227
72 h	0.506±0.004*	0.307±0.013**	0.389±0.912**	0.784±0.141

HCC and MIHA cells were treated with I-ATXP for 24 h, 48 h, and 72 h. The half inhibition concentration IC50 was obtained by the Probit method. The experimental data was obtained by averaging three independent parallel experiments. Compared with MIHA, *P < 0.05, **P < 0.001.

bition) of I-ATXP on HepG2, SMMC7721, HKCI-C3 HCC cell line, and MIHA cells for 24 h, 48 h, and 72 h. The results of concentration IC50, using SPSS 22.0 Probit method to calculate IC50 value, are shown in **Table 1**. The data showed that IC50 values of the three types of liver cancer cells were significantly lower than those of MIHA ($P < 0.05$), indicating that the toxicity of I-ATXP to the three liver cancer cells was significantly greater than that of non-cancer cells. After 48 hours of drug action, the IC50 value of HepG2 cells was significantly lower than that of MIHA cells ($P < 0.05$), while SMMC7721 and HKCI-C3 cells were not significantly different from MIHA cells ($P > 0.05$). The data was a show that after 24 h, 48 h, and 72 h of treatment with different concentrations of I-ATXP (0.125-1 mg/ml), the IC50 values of the three types of liver cancer cells were all lower than the IC50 value of MIHA, especially after 24 hours of drug action. The IC50 value of MIHA cells was 5.079±0.317 mg/ml, which is twofold more than that of the other three liver cancer cells. The SMMMC7721 cells (IC50 0.307 mg/ml) and HKCI-C3 cells (IC50 0.389 mg/ml) were more sensitive than HepG2 cells (IC50 0.506 mg/ml) to I-ATXP-induced inhibition of proliferation at 72 hours. Furthermore, I-ATXP inhibited HepG2, SMMC7721, and HKCI-C3 of HCC proliferation in a dose- and time-dependent manner. In the SMMC7721 cells and HKCI-C3 cells, a sharp decrease in cell viability was observed with 0.125 mg/ml I-ATXP for 72 hours. This result indicates that I-ATXP can selectively act on liver cancer cells and exert a specific cytotoxic effect, indicating that I-ATXP may have higher clinical application safety (**Table 1**).

I-ATXP inhibits the proliferation of HCC cells

We used the CCK-8 assay to demonstrate the inhibitory effect of I-ATXP on the proliferation of HCC cells. The data showed that I-ATXP inhibited HepG2, SMMC7721, and HKCI-C3 cells; as a control, it immortalized hepatocyte cell line MIHA. Cells were incubated with I-ATXP (0.125 mg/ml, 0.25 mg/ml, 0.5 mg/ml, and 1 mg/ml), with 5-Fluorouracil (5-Fu, 0.2 mg/ml) as a positive control at varying dosage for 72 hours, and proliferation was measured by CCK-8 assay. Results of three independent experiments showed that after different concentrations of I-ATXP acted on HepG2, SMMC7721, HKCI-C3, and MIHA cells for 72 h, the inhibitory effect of I-ATXP on the four types of hepatocytes was concentration-dependent. The survival rate was gradually decreased. The data showed that the inhibitory effect of I-ATXP on liver cancer cells HepG2, SMMC7721, and HKCI-C3 was significantly stronger than that of non-carcinoma-active immortalized liver cells MIHA. As the concentration and duration of action increased, the survival rate of the three types of hepatocellular carcinoma cells in the I-ATXP treatment group was significantly reduced.

The results have also shown that the modified Aitongxiao Recipe has a significant inhibitory effect on the proliferation of liver cancer cells HepG2, SMMC7721, and HKCI-C3 and is related to the time and concentration of the drug. Compared with the positive drug fluorouracil (5-Fu), I-ATXP was more selective and specific in inhibiting cell proliferation (**Figure 1**).

I-ATXP induces cell cycle arrest in HCC cells

Based on the above data, we know that I-ATXP can inhibit the proliferation of HepG2, SMMC-7721, and HKCI-C3 of HCC cells. Studies have shown that drugs inhibit tumor cell growth by promoting cell apoptosis and inhibiting the cell cycle. Therefore, this study used flow cytometry, Annexin V-FITC/PI double staining method, and PI single staining method to detect the effect of I-ATXP on the apoptosis and cell cycle of HCC cells. To discuss and analyze the possible mechanism of I-ATXP inhibiting the proliferation of HCC cells, we determine the effect of I-ATXP on the cell cycle arrest in HepG2, SMMC7721, and HKCI-C3 HCC cells, and the cell cycle distribution was investigated by flow

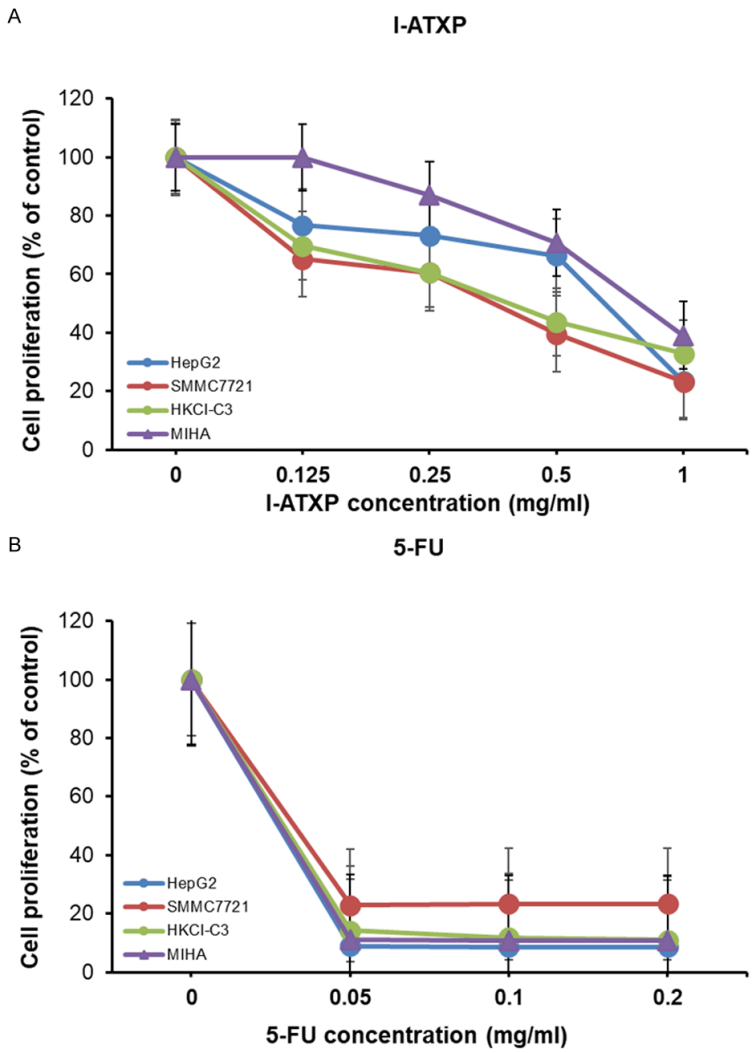

Figure 1. I-ATXP inhibits proliferation of HepG2, SMMC7721, and HKCI-C3 human hepatocellular carcinoma cell lines and MIHA immortalized hepatocyte cell line. Cells were incubated with I-ATXP, 5-Fluorouracil (5-Fu) as a positive control at varying dosage for 72 hours, and proliferation was measured by CCK-8 assay. The results of three independent experiments are shown. (A) HepG2, SMMC7721, HKCI-C3, and MIHA cells were treated with various doses I-ATXP (0, 0.125, 0.25, 0.5, and 1 mg/ml) for 72 h followed by CCK8 assay, and (B) HepG2, SMMC7721, HKCI-C3, and MIHA cells were treated with various doses of 5-FU (0, 0.05, 0.1, and 0.2 mg/ml) for 72 hours followed by CCK8 assay.

cytometry. Compared with the untreated cells, the G0/G1 phase ratios in HepG2, SMMC7721, and HKCI-C3 of HCC cells were significantly higher than those in the untreated group ($P < 0.0001$). As shown in **Figure 2A**, compared with the blank control group, after 24 h of I-ATXP (0.125-1 mg/ml) in HepG2 cells at different concentrations, the proportion of G0/G1 phase increased significantly ($P < 0.05$). The proportion of HepG2 cells in the G0/G1 phase increased significantly from 49.463±3.749% in the blank control group to 59.917±2.533% in the high-dose group (1 mg/ml, $P < 0.0001$), and this ratio is drug concentration-dependent. The proportion of G0/G1 phase increased with the increase of drug concentration. It showed that I-ATXP has an evident cycle inhibitory effect on liver cancer cell HepG2 and can induce cell cycle arrest in G0/G1 phase. As shown in **Figure 2B**, compared with the blank control group, the ratio of G0/G1 phase increased significantly after different concentrations of I-ATXP (0.125-1 mg/ml) were treated SMMC7721 cells for 24 h ($P < 0.001$). The proportion of SMMC7721 cells in the G0/G1 phase increased significantly from 41.010±1.156% in the blank control group to 65.923±3.525% in the high-dose group (1 mg/ml), and this ratio was drug concentration-dependent. The proportion of G0/G1 phase increased with the increase of drug concentration. It showed that I-ATXP has an evident cycle inhibitory effect on liver cancer cell SMMC7721 and can induce G0/G1 phase cycle arrest in cells. As shown in **Figure 2C**, compared with the blank control group, after different concentrations of I-ATXP (0.125-1 mg/ml) treated HKCI-C3 cells for 24 h, the proportion of G0/G1 phase was significantly higher ($P < 0.0001$) than that of the blank control group. The proportion of HKCI-C3 cells in the G0/G1 phase increased significantly from 40.417±1.948% in the blank control group to 55.863±2.639% in the high-dose group (1 mg/ml) and showed a drug concentration-dependent. The proportion of G0/G1 phase increased with the increase of drug concentration. It showed that I-ATXP has an evident cycle inhibitory effect on liver can-

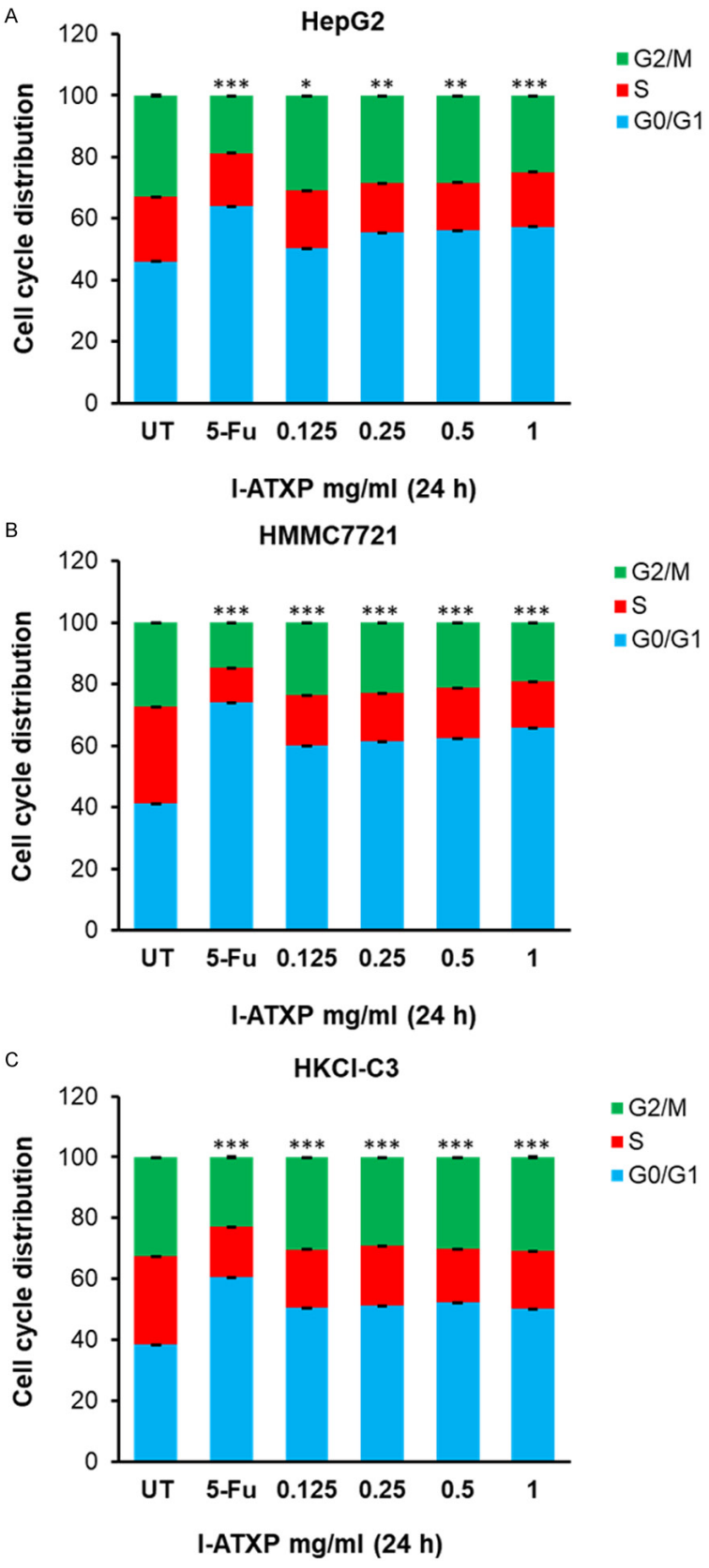

Figure 2. I-ATXP antagonist and 5-FU chemotherapy induced cell cycle arrest on G0/G1 phase in HepG2, SMMC-7721, and HKCI-C3 liver cancer cells. Cells were treated with dosages of 0.125 mg/ml, 0.25 mg/ml, 0.5 mg/ml, and 1 mg/ml of I-ATXP mock as negative control, and 0.2 mg/ml 5-Fu as positive control. Cells were then incubated at 37°C for 24 hours and were assayed by Flow Cytometry, indicating the percentage of (A) HepG2 cells, (B) SMMC-7721 cells, and (C) HKCI-C3 cells in various cell cycle phases. The results of three independent experiments are shown. Significant differences relative to untreated control are indicated as follows: $*P < 0.05$, $**P < 0.005$, $***P < 0.0005$ *and* $****P < 0.00005$.

cer cell HKCI-C3 and can induce G0/G1 phase cycle arrest in cells. The results demonstrated that I-ATXP could induce cell cycle arrest at the G0/G1 phase in HCC cells (**Figure 2**).

I-ATXP induced cell apoptosis in HCC cells

The effect of I-ATXP on the induction of cell apoptosis in hepatoma cells was measured by PI-Annexin V double staining. It can be seen from **Figure 3A** that compared with the blank control group, after 24 hours of treatment of cells with different concentrations of I-ATXP (0.125-1 mg/ml), the percentage of apoptotic cells (LR+UR) in HepG2 to all cells was significantly higher than the blank control ($P < 0.001$). In particular, the rate of HepG2 cell apoptosis increased significantly from 9.8% in the blank control group to 31.95% in the high-dose group (1 mg/ml). This result shows that I-ATXP can induce cell apoptosis in HepG2 hepatoma cells. As shown in **Figure 3B**, compared with the blank control group, the apoptotic cells (LR+UR) of SMMC7721 accounted for the proportion of all cells in the medium and high-dose

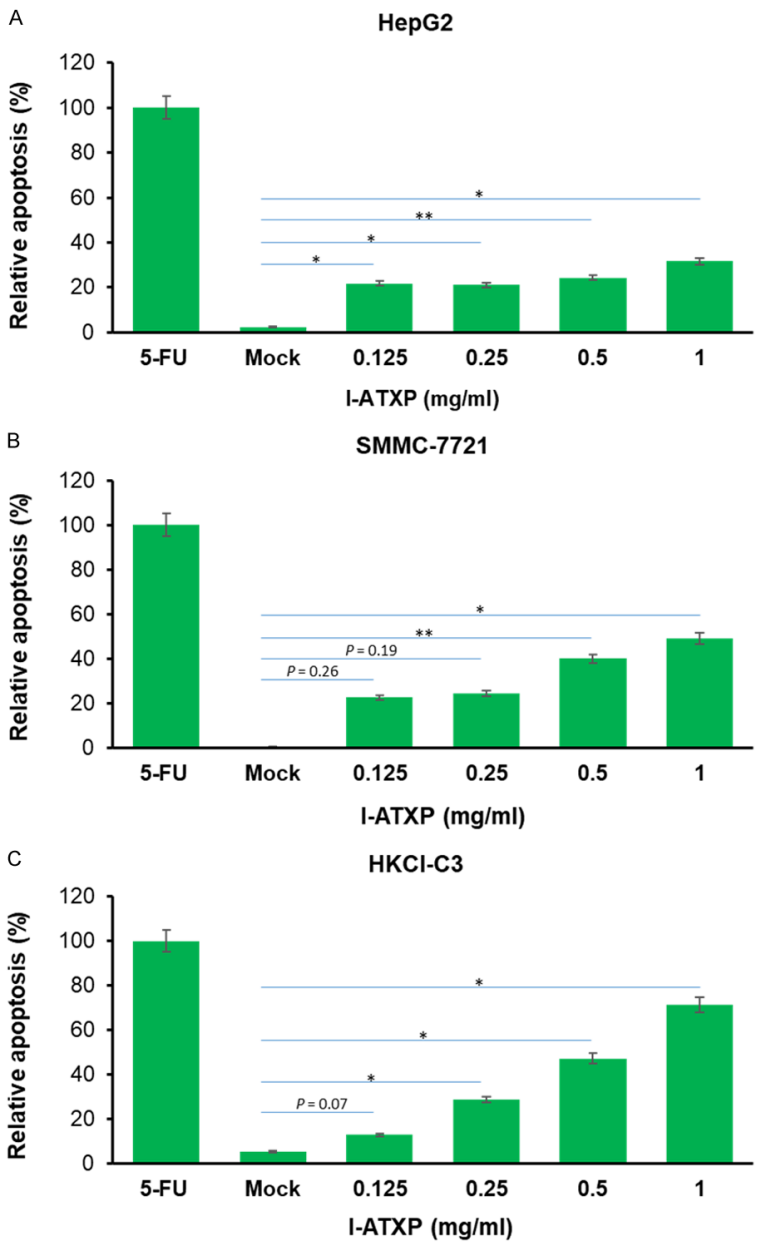

Figure 3. I-ATXP induced the apoptosis of HepG2, SMMC-7721 and HKCI-C3 liver cancer cells. Percentage of apoptotic cells (A) HepG2 cells, (B) SMMC-7721 cells, and (C) HKCI-C3 cells, as determined by Annexin V-FITC assay of cells treated with various concentrations of ATX for 24 hours. Error bars represent mean ± SD of four independent experiments. Significant differences relative to mock are indicated as follows: $*P < 0.05$, $**P < 0.005$.

groups I-ATXP (0.5-1 mg/ml) for 24 h. The ratio was significantly higher than that of the blank control ($p < 0.05$); there was no significant difference between the lowest and low-dose groups (0.125-0.25 mg/ml). The proportion of SMMC7721 cell apoptosis increased significantly from 0.15% in the blank control group to 24.1% in the high-dose group (1 mg/ml). It shows that I-ATXP can induce cell apoptosis of SMMC7721 liver cancer cells. The results in **Figure 3C** show that, compared with the blank control group, after 24 hours of treatment of cells with different concentrations of I-ATXP (0.125-1 mg/ml), the proportion of apoptotic cells (LR+UR) in HKCI-C3 to all cells was equal. It was higher than the blank control and is drug concentration dependent. Among them, there was no significant difference between the low-dose group (0.125 mg/ml) and the blank control group ($P > 0.05$), while the higher-dose group (0.25 mg/ml, 0.5 mg/ml, 1 mg/ml) increased significantly ($P < 0.05$). In particular, the percentage of HKCI-C3 cell apoptosis increased significantly from 5.35% in the blank control group to 22.8% in the high-dose group (1 mg/ml). It shows that I-ATXP can induce apoptosis of hepatoma cells HKCI-C3, which is drug concentration-dependent.

Effect of I-ATXP on the secretion of exosomes in HCC cells

The research above found that I-ATXP has a proliferation inhibitory effect on HCC cells and can inhibit liver cancer cell proliferation by inducing apoptosis and cycle arrest of liver cancer cells. Tumor cell-derived exosomes play a significant biological role in the development of cancer. They can transmit the molecular and genetic information of tumor cells to normal cells located close or distant. They can also change these target cell phenotypes and functions, promoting tumor growth and metastasis [44]. Therefore, we speculated whether I-ATXP could change the RNA or protein carried by liver can-

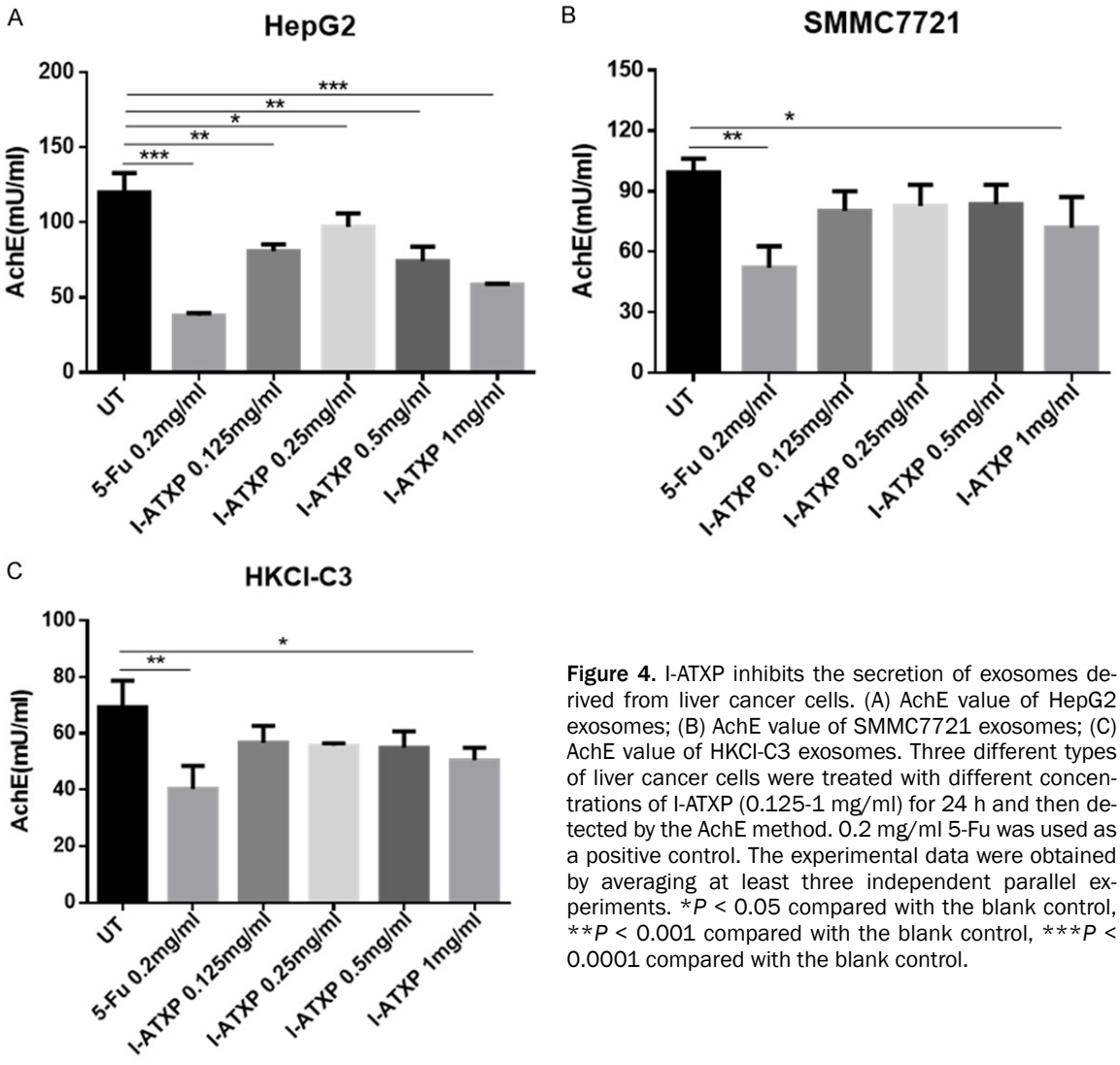

Figure 4. I-ATXP inhibits the secretion of exosomes derived from liver cancer cells. (A) AchE value of HepG2 exosomes; (B) AchE value of SMMC7721 exosomes; (C) AchE value of HKCI-C3 exosomes. Three different types of liver cancer cells were treated with different concentrations of I-ATXP (0.125-1 mg/ml) for 24 h and then detected by the AchE method. 0.2 mg/ml 5-Fu was used as a positive control. The experimental data were obtained by averaging at least three independent parallel experiments. *$P < 0.05$ compared with the blank control, **$P < 0.001$ compared with the blank control, ***$P < 0.0001$ compared with the blank control.

cer cell-derived exosomes, thereby affecting information transmission and regulating liver cancer cells' growth and proliferation. Therefore, the acetylcholinesterase (AchE) experiment was used to detect the changes in the number of exosomes secreted by I-ATXP in HCC cells. Western blot was used to detect the changes in the expression of exosome-specific proteins CD63 and Alix and to explore the effects of I-ATXP on the secretion of exosomes derived from liver cancer cells. This also lays the foundation for other lingering I-ATXP mechanisms on liver cancer cells.

I-ATXP blocks exosomes release from HCC cells-derived exosomes: We used the AchE measurement to quantify exosome secretion from different liver cancer cells [45]. As shown in **Figure 4**, after 24 h of I-ATXP (0.125-1 mg/ml) at different concentrations, the AchE values of cell-derived exosomes were significantly lower than the blank control group ($P < 0.01$). Compared with the blank control group, the AchE value of HepG2 cell exosomes was significantly lower than that of the blank control group ($P < 0.05$): from about 120 mU/ml in the blank control group to 58 mU in the high-dose group (1 mg/ml)/ml; the AchE value of SMMC-7721 exosomes in the high-dose drug group was significantly lower than that of the blank control group ($P < 0.05$) while there was no significant difference in the other groups ($P > 0.05$). About 99 mU/ml in the blank control group was significantly reduced to about 72 mU/ml in the high-dose group (1 mg/ml); the AchE value of HKCI-C3 exosomes in the high-

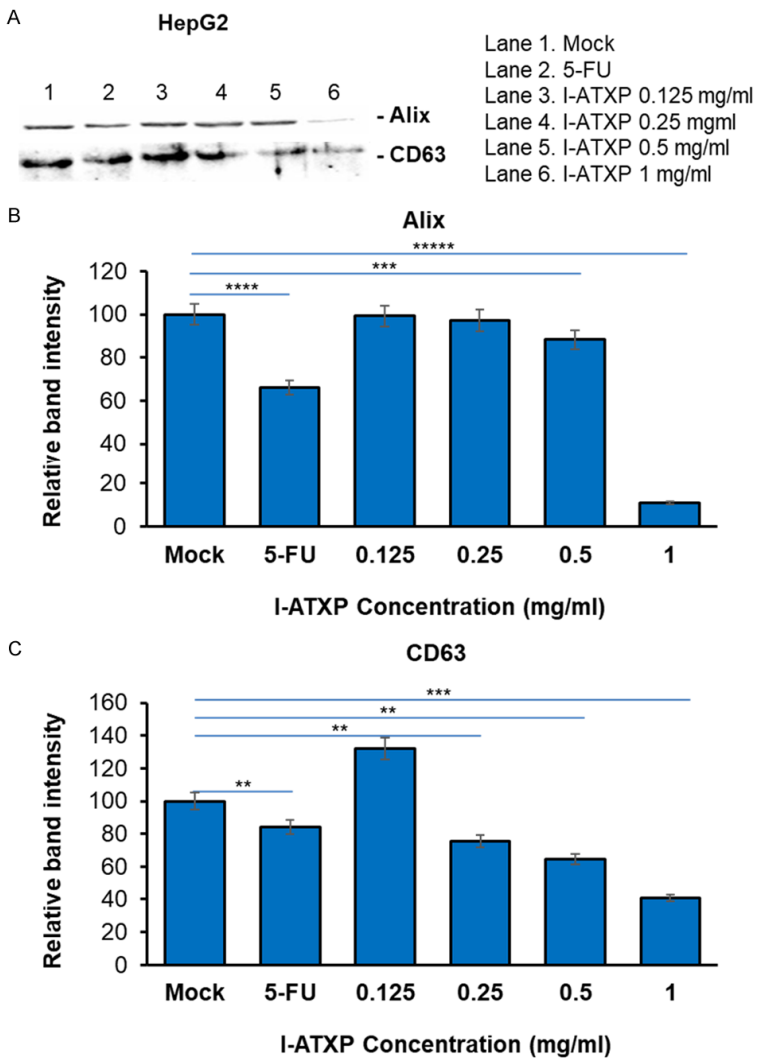

Figure 5. Exosome production by HepG2 liver cancer cells was decreased by I-ATXP treatment. Cells were treated with 0.125 mg/ml, 0.25 mg/ml, 0.5 mg/ml, and 1 mg/ml of I-ATX for 24 hours. (A) Expression of exosome proteins by Western blot analysis; (B) densitometry analysis showing the relative intensity of bands of Alix; and (C) densitometry analysis showing relative intensity of bands of CD63. Data represent the mean ± SD of three independent experiments. Significant differences relative to treatment with peptide are indicated as follows: $^{**}P < 0.001$, $^{***}P < 0.0001$, $^{***}P < 0.00001$, $^{****}P < 0.00001$ and $^{*****}P < 0.000001$.

dose drug group was significantly lower than that of the blank control group ($P < 0.05$), but there was no significant difference in the other groups ($P > 0.05$). It was significantly reduced from about 69 mU/ml in the blank control group to about 50 mU/ml in the high-dose group (1 mg/ml). It can be seen that I-ATXP can reduce the AchE value of exosomes derived from three types of liver cancer cells. Compared with 5-Fu, under the existing experimental conditions, the I-ATXP treatment group inhibitory effect was weaker.

I-ATXP reduces exosome protein expression of Alix and CD63 protein: To further determine the effect of I-ATXP on the secretion of exosomes derived from liver cancer cells, we used Western blot to detect exosome-specific proteins: Alix and CD63. As shown in **Figure 5**, after 24 hours of different concentrations of I-ATXP (0.125-1 mg/ml) on the cells, the exosomes derived from HepG2 cells could express the Alix's exosome-specific proteins and CD63. Compared with the blank control group, Alix and CD63 protein expression in HepG2 cells decreased with drug concentration. Among them, the expression of HepG2 cell exosome specific protein Alix did not differ from the blank control group at relatively low concentrations of 0.125-0.5 mg/ml ($P > 0.05$). It was significant in the high-dose group (1 mg/ml) and lower than the blank control group ($P < 0.0001$). The expression of the exosome-specific protein, CD63, in the low-dose group (0.125 mg/ml) was significantly higher than the blank control group ($P < 0.001$), and at 0.25-1 mg/ml, it was reduced considerably with time ($P < 0.001$). As shown in **Figure 6**, after different concentrations of I-ATXP (0.125-1 mg/ml) acted on the cells for 24 h, the exosomes derived from SMMC7721 cells could express the exosome-specific proteins, Alix and CD63. Compared with the blank control group, Alix and CD63 protein expression in SMMC7721 cells was significantly reduced ($P < 0.0001$), and in a concentration-dependent manner, the expression of SMMC7721 exosome-specific proteins, Alix and CD63, decreased with increased drug concen-

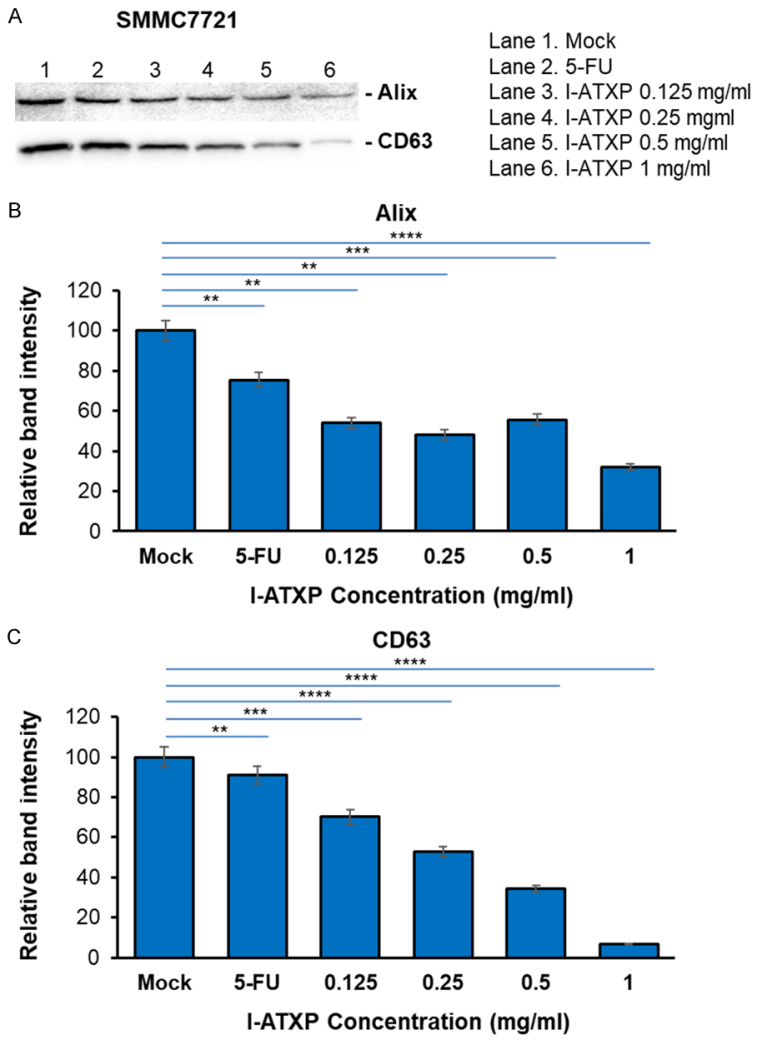

Figure 6. Exosome production by SMMC7721 liver cancer cells was decreased by I-ATXP treatment. Cells were treated with 0.125 mg/ml, 0.25 mg/ml, 0.5 mg/ml, and 1 mg/ml of ATX for 24 hours. (A) Expression of exosome proteins by Western blot analysis; (B) densitometry analysis showing the relative intensity of bands of Alix; and (C) densitometry analysis showing the relative intensity of bands of CD63. Data represent the mean ± SD of three independent experiments. Significant differences relative to treatment with peptide are indicated as follows: $^{**}P < 0.001$, $^{***}P < 0.0001$ and $^{****}P < 0.00001$.

tration. This result indicates that I-ATXP can inhibit the expression of specific proteins, Alix and CD63, in exosomes derived from SMMC-7721 liver cancer cells. As shown in **Figure 7**, after different concentrations of I-ATXP (0.125-1 mg/ml) acted on the cells for 24 h, the exosomes derived from HKCI-C3 cells could express the exosome-specific proteins Alix and CD63. Compared with the blank control group, Alix and CD63 protein expression in HKCI-C3 cells decreased with drug concentration. The expression of exosome specific protein Alix did not decrease in a dose in a dose specific manner in HKCI-C3 cells. However, the expression of exosome-specific protein CD63 in HKCI-C3 cells was dose-specific. At the lowest dose (0.125 mg/ml) it was similar to that of the blank control group ($P > 0.05$) and was significantly reduced at 0.25-1 mg/ml ($P < 0.001$).

The role of HCC derived exosomes in HCC cells

Exosomes play an important role in the occurrence and development of tumors, and the various contents (DNA, RNA, and proteins) contained in them can also play different roles in cells. They can regulate a variety of signal pathways. As the human body's first line of defense against pathogens and anti-tumors, the activation of innate immune receptors TLRs can initiate the activation of downstream signaling pathways, regulating the expression of various cytokines, etc. In this study, we used exosomes derived from HCC cells. We identified their effects on the proliferation, invasion, migration, and other biological properties of HCC cells and their impact on the expression of innate immune receptor TLR8 and it is signaling pathway-related molecules and downstream cytokines in HCC cells-the regulating effect.

HCC derived exosome increases the wound-healing rate in HCC cells: Our data showed that the lateral migration rate of (*a*) HepG2 and SMMC-7721 cells treated with different concentrations of liver cancer cell exosomes (10 and 20 μg/ml) on HepG2 and SMMC-7721 cells for 12 hours was significantly increased ($P < 0.05$) and increased as the concentration of tumor exosome increased. (*b*) Compared with the blank control group, the number of migrations of HepG2 cells was significantly increased after the addition of exosomes ($P < 0.05$); at the same time, the invasion ability of cells was

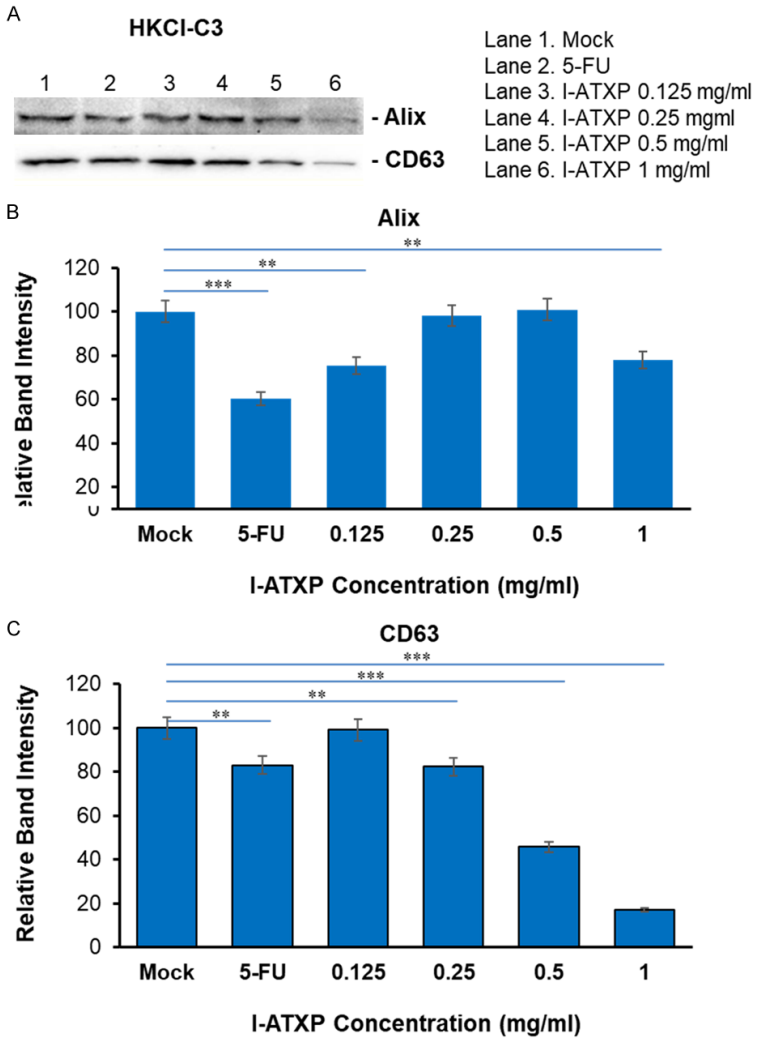

Figure 7. Exosome production by HKCl-C3 liver cancer cells was decreased by I-ATXP treatment. Cells were treated with 0.125 mg/ml, 0.25 mg/ml, 0.5 mg/ml, and 1 mg/ml of ATX for 24 hours. (A) Expression of exosome proteins by Western blot analysis; (B) densitometry analysis showing the relative intensity of bands of Alix; and (C) densitometry analysis showing the relative intensity of bands of CD63. Data represent the mean ± SD of three independent experiments. Significant differences relative to treatment with peptide are indicated as follows: $^{**}P < 0.001$ and $^{***}P < 0.0001$.

also significantly enhanced ($P < 0.05$). (c) After different concentrations of HCC-derived exosomes acted on HepG2 and SMMC-7721 cells for 12 hours, there was no significant change in the proliferation of liver cancer cells in comparison to the blank control group ($P > 0.05$) (**Figures 8** and **9**).

HCC derived exosome induces migration and invasion in HCC cells: The above scratch results showed that 10 μg/ml tumor exosome caused a significant increase in the lateral mobility of HCC cells. Therefore, we used 10 μg/ml and 20 μg/ml exosomes for migration assay (**Figure 10A**). The number of HepG2 cells that migrated through the chamber was significantly increased compared with the control group. The number of cells in the control group was 98±9. In the 10 μg/ml exosome group, the number of cells that migrated through the chamber was about 187±20. At a 20 μg/ml exosome concentration, the number of cells that passed through was about 160±18, and the number of cells increased significantly ($P < 0.05$) (**Figure 10C**). In the invasion assay (**Figure 10B**), the number of HepG2 cells in the control group was 109±14. In the 10 μg/ml exosome group, the number of cells was 198±27. In the 20 μg/ml exosome group, the number of invading cells was about 191±12, and the number of invading cells also increased significantly ($P < 0.05$) (**Figure 10D**). However, under the same conditions, SMMC-7721 cells failed to pass through the bottom of the chamber successfully, showing the lack of ability to migrate and invade (data not shown).

Exosome morphological characteristics were identified by transmission electron microscopy (TEM)

Transmission electron microscopy of isolated exosomes. Exosomes were isolated from the culture media of HepG2 cells using an exosome isolation kit. The isolates were examined by electron microscopy (**Figure 11**), using negative staining with uranyl acetate to verify that the isolated structures were exosomes. The electron images depicted rounded structures with a size range of 50-100 nm in diameter and a cup-shaped morphology, which con-

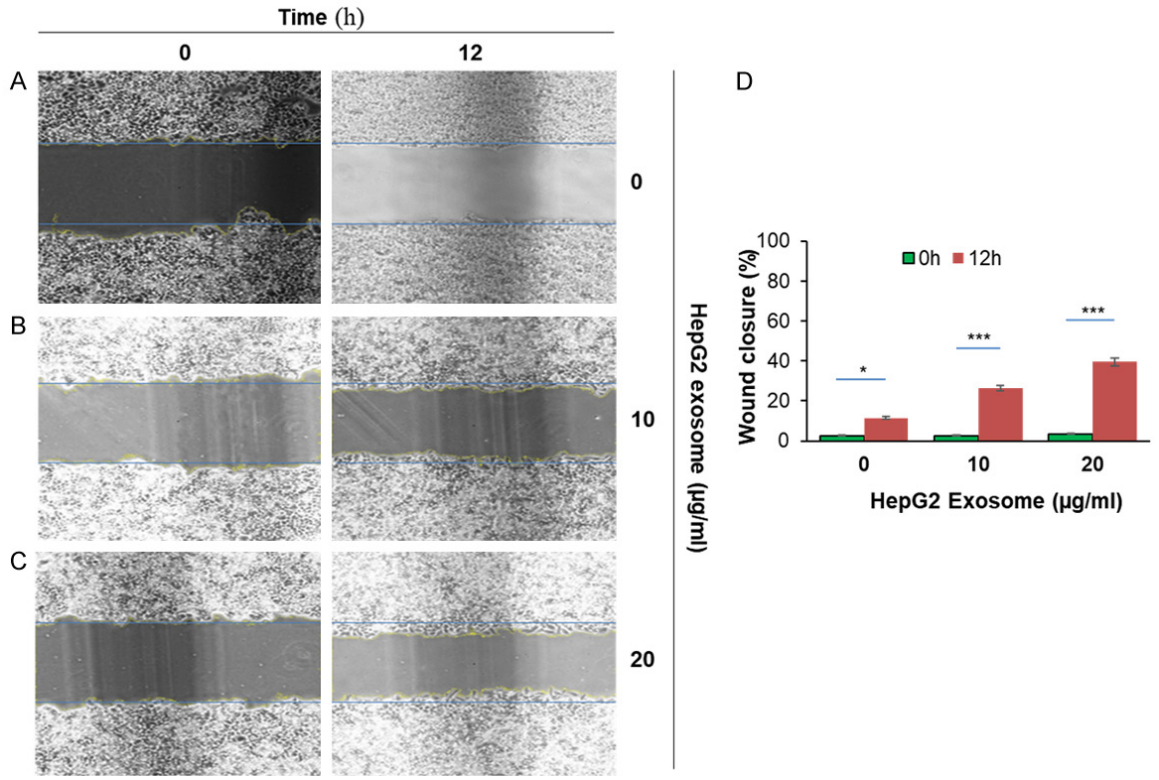

Figure 8. HepG2 liver cancer cells-derived exosome induced migration in HepG2 cells. 1×10^6 HepG2 cells were added into 6-well plates for 24 hours until a monolayer formed. Cells were treated with 20 μg/ml of Mitomycin for 3 hours. On the cell surface, we drew a vertical line using a 200 μl pipet and washed it with PBS three times. Cells were treated with various concentrations of HepG2 derived exosome (10 μg/ml and 20 μg/ml) at 37°C for 12 hours and were monitored to determine percent closure by microscopy. (A) HepG2 cells were treated with PBS for 0 hour and 12 hours; (B) HepG2 cells were treated with 10 μg/ml of exosomes for 0 hour and 12 hours; (C) HepG2 treated with 20 μg/ml of exosomes for 0 hour and 24 hours, and (D) cells percent closures were obtained after cells were treated with exosomes for 12 hours (11.5%, 26.34%, and 39.5%). Significant difference relative to untreated control are indicated as follows: *$P < 0.01$, ***$P < 0.0004$. The images were taken via microscopy: magnification, ×100.

firmed the successful isolation of exosomes according to previously described exosome characteristics.

Discussion

Hepatocellular carcinoma (HCC) is one of the most common malignancies worldwide. The present study was undertaken to determine whether exosomes can alter cancer cells' metastatic potential by mechanisms that may include the roles of exosomes in signal transduction pathways between hepatoma cells. Exosomes are vesicles of about 30-100 nm diameter secreted by a variety of living cells and typically contain cellular proteins and RNA. These ubiquitous nanoparticles in the body can fuse with the cell membranes of various tissues, thus participating in the exchange of materials and information between cells. They play an important role in a variety of physiological and pathological processes. Exosomes are involved in important biological processes such as immune response, apoptosis, angiogenesis, inflammation, and coagulation. Cells deliver signaling molecules to distant tissues or cells by secreting exosomes.

Studies have shown that substances delivered by exosomes are involved in growth, metastasis, and angiogenesis in liver cancer and inhibit the growth of liver cancer by blocking the signaling pathway of liver cancer cells. In this study, we aimed to reveal the significance of exosomes in the development, diagnosis, and treatment of HCC, which might help us further elucidate the mechanism of exosomes in HCC and promote the use of exosomes in the clinical diagnosis and treatment of HCC. In addition, exosome substances could also be used

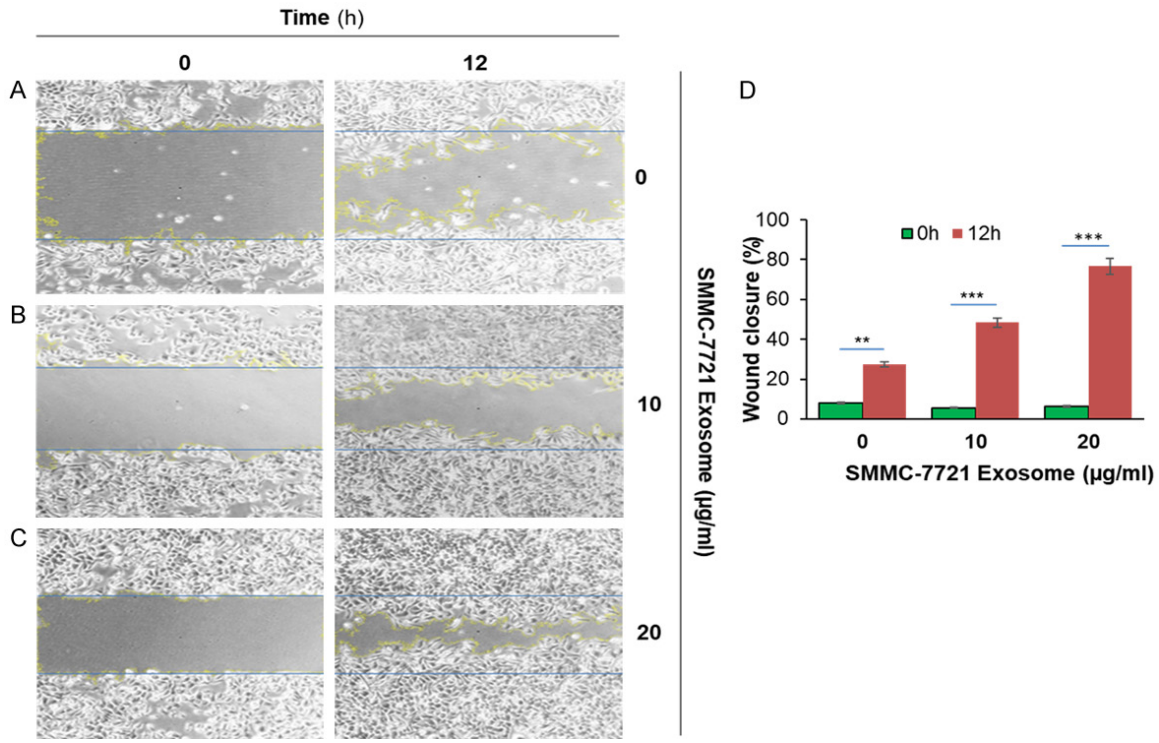

Figure 9. SMMC-7721 liver cancer cells derived exosome induced migration in SMMC-7721 cells. 1×10^6 SMMC-7721 cells were added into 6-well plates for 24 hours until a monolayer formed. Cells were treated with 20 μg/ml of Mitomycin for 3 hours. On the cell surface, we drew a vertical line using 200 μl pipet and washed it with PBS three times. Cells were treated with various concentrations of SMMC-7721 derived exosome (10 μg/ml and 20 μg/ml) at 37°C for 12 hours and were monitored to determine percent closure by microscopy. (A) SMMC-7721 cells were treated with PBS for 0 hour and 12 hours; (B) SMMC-7721 cells were treated with 10 μg/ml of exosomes for 0 hour and 12 hours; (C) SMMC-7721 cells were treated with 20 μg/ml of exosomes for 0 hour and 12 hours, and (D) cells percent closures were obtained after cells were treated with exosomes for 12 hours (23.37%, 48.38%, and 76.6%). Significant difference relative to untreated control are indicated as follows: $**P < 0.003$, $***P < 0.0006$. The images were taken via microscopy: magnification, ×100.

as markers for the early detection of liver cancer.

To the best of our knowledge, the present study is the first to conduct protein profiling of exosomes from different HCC cell origins, identifying protein associated with HCC metastasis and recurrence. Collectively, these data may provide the foundation for further studies into the regulatory role of exosomes in cell-cell communication in HCC and other cancers.

The inhibitory effect of I-ATXP on the proliferation of liver cancer cells

Traditional Chinese medicine treatment is an essential part of comprehensive tumor treatment. Synthesizing the pharmacological research basis of the Aitongxiao prescription, as well as the results of clinical, animal, and cell research in the early stage, confirmed that Aitongxiao prescription has the effect of promoting HCC cell apoptosis and inhibiting the growth, invasion, and metastasis of HCC cells [39-41, 53]. To better exert the drug's efficacy, we made further additions, subtractions, and improvements to the Aitongxiao recipe based on the clinical efficacy in recent years and obtained an improved Aitongxiao recipe. To explore and explain the mechanism of modified Aitongxiao decoction in the treatment of HCC, this study used in vitro cell culture method and CCK-8 method to analyze the proliferation inhibitory effect of modified Aitongxiao decoction on different liver cancer cells: HepG2, SMMC7721, and HKCI-C3.

Four types of cells were selected in this study. HepG2, SMMC7721, and HKCI-C3 are hepatocellular carcinoma cells with cancerous activity

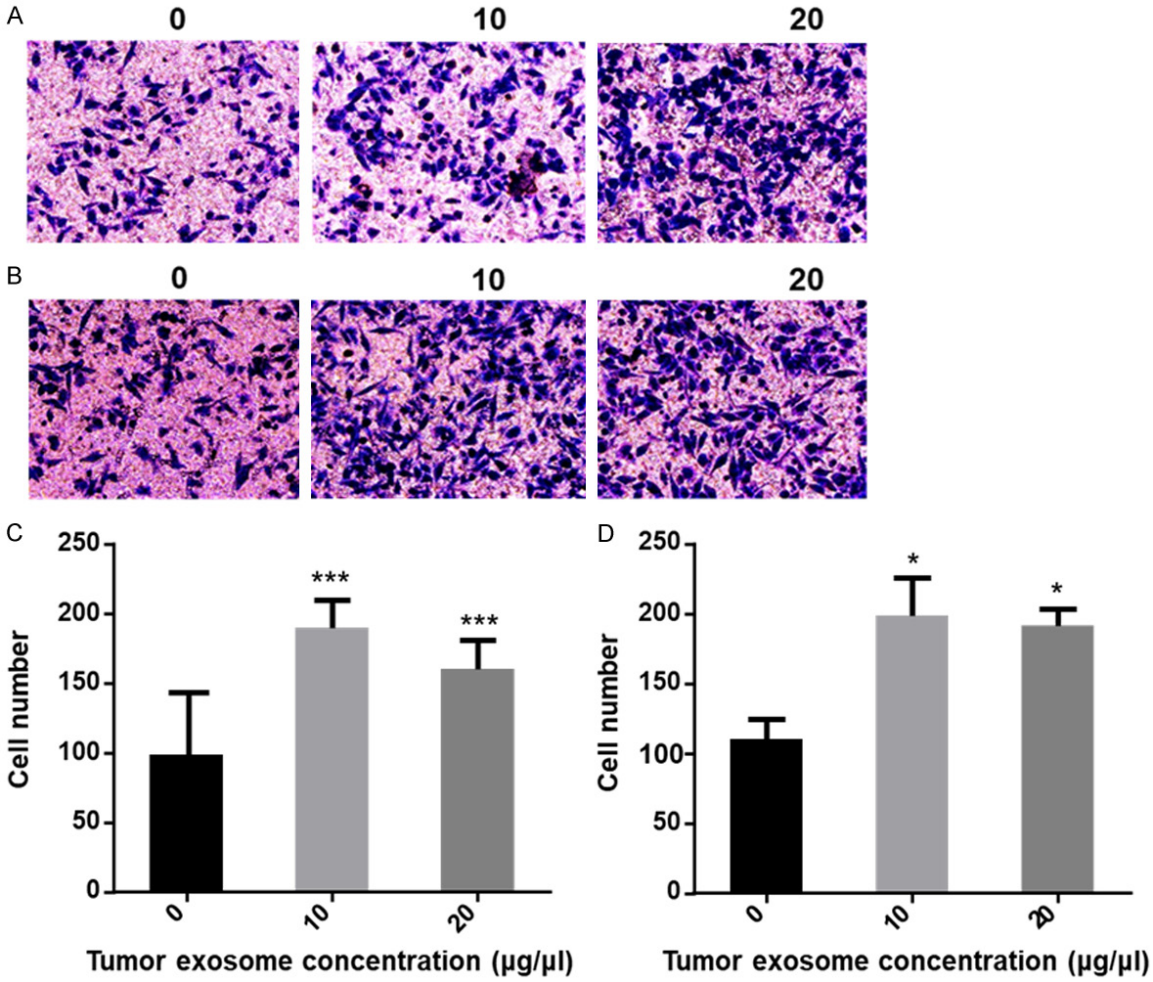

Figure 10. Different concentration of tumor exosome increases the migration and invasion in HepG2 cells. (A) Image of migratory cells; (B) Image of invasion cells. The images were taken via fluorescence microscopy. Magnification, ×200; (C) Error bars represent the standard deviation of three independent experiments. ***$P < 0.001$ compared to the control of the migratory cells; (D) Error bars represent standard deviation of three independent experiments. *$P < 0.05$ compared to the control of invasion cells.

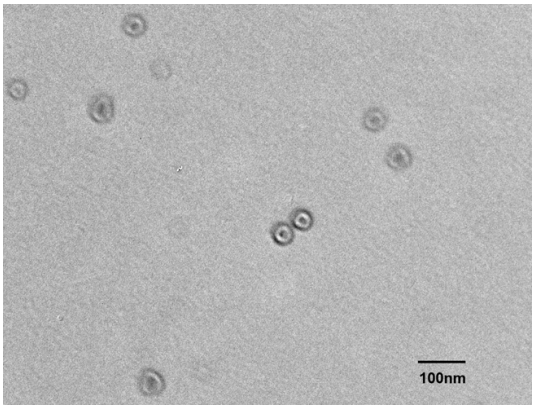

Figure 11. Transmission electron microscopy (TEM) of exosomes isolated from supernatants of HepG2, a liver cancer cell line. Exosomes isolated by differential centrifugation, ultrafiltration, and size exclusion chromatography were placed on copper grids and stained with 1% uranyl acetate and examined. Note their vesicular morphology and the size range, which does not exceed 100 nm.

from human liver cancer tissues. We decided the immortalized hepatocytes, MIHA, without cancer activity [42]. By studying a variety of liver cancer cells, we can further determine whether the inhibitory effect of I-ATXP on liver cancer cells is universal. By comparing liver cancer cells with immortalized cells without cancer activity, we can further determine whether I-ATXP inhibits liver cells.

The basis of the anti-tumor effect of drugs is their selectivity to different cells. The drug tox-

icity of I-ATXP has a specific selectivity. We used the CCK-8 method to detect the growth inhibitory effect of I-ATXP on hepatocarcinoma cells HepG2, SMMC7721, and HKCI-C3, and non-carcinomatous immortalized liver cell line, MIHA cells. When the drug acts for 24 hours, its IC50 for sensitive cell liver cancer cells HepG2, SMMC7721, and HKCI-C3 was 2.189± 0.472 mg/ml, 2.519±1.101 mg/ml, 1.827± 0.326 mg/ml, respectively. For the non-carcinogenic immortalized hepatocytes, the concentration of MIHA's half inhibition rate was 5.079±0.317 mg/ml, indicating that MIHA cells were less sensitive to the effects of I-ATXP drugs than other cells. Although the positive drug fluorouracil (5-Fu) has a more substantial inhibitory effect on the four types of cells than I-ATXP, it has no selective effect on cell proliferation.

We tested the cytotoxic effects of I-ATXP on liver cancer cells HepG2, SMMC7721, HKCI-C3, and non-carcinomatous immortalized liver cells, MIHA, through cell proliferation experiments. The results showed that the inhibitory effect of I-ATXP on the growth of three types of hepatocellular carcinoma cells was time- and concentration-dependent. As the concentration and duration of action increased, the survival rates of the three types of hepatocellular carcinoma cells in the I-ATXP treatment group were significantly reduced. The inhibitory effect of I-ATXP on different cells was selective. It was resistant to non-cancerous active immortal liver cells, MIHA. The inhibitory effect of the three kinds of liver cancer cells was lower. From this, we speculate that I-ATXP has an anti-tumor-specific impact.

The research results in this chapter show that the modified Aitongxiao Recipe has a significant inhibitory effect on the proliferation of liver cancer cells HepG2, SMMC7721, and HKCI-C3 and is related to the time and concentration of the drug. Compared with the positive drug fluorouracil (5-Fu), the Modified Aitongxiao recipe is more selective and specific in inhibiting cell proliferation. This also shows the advantage of traditional Chinese medicine in treating tumors and provides experimental evidence for clinical treatment.

Effect of I-ATXP on apoptosis and cell cycle of liver cancer cells

We have confirmed that I-ATXP can inhibit the growth and proliferation of liver cancer cells, HepG2, SMMC7721, and HKCI-C3, and induce their death through cell proliferation tests. Drugs inhibit tumor cell growth mainly by promoting cell apoptosis and inhibiting the cell cycle. As a result, we used Annexin V-FITC/PI double staining to detect whether I-ATXP induced apoptosis of hepatoma cells HepG2, SMMC7721, and HKCI-C3. The occurrence and development of tumors are related to the excessive proliferation of cells and the slowing down of cell death. A disorder of apoptosis must accompany the process of tumor occurrence. The concept of cell apoptosis, which refers to a kind of programmed cell death, was first proposed in 1972 by Kerr [52] and others. Its morphological and biological characteristics are different from cell necrosis, and it is generally considered to be the maintenance of organisms-one of the essential mechanisms for constant homeostasis. Disruption of apoptosis, the active and orderly process of cell self-destruction, will lead to abnormal cell development, which will cause and accelerate the occurrence and deterioration of tumors.

The test results showed that the ratio of apoptotic cells (LR+UR) of SMMC7721 and HKCI-C3 increased significantly with the increased concentration of I-ATXP. Among them, in the concentration range of 0.125-1 mg/ml, the inhibitory effect of I-ATXP on SMMC7721 and HKCI-C3 was concentration-dependent. The apoptosis rate of SMMC7721 cells was significantly increased from 0.15% in the blank control group to 24.1% in the 1 mg/ml group. The percentage of HKCI-C3 cell apoptosis increased significantly from 5.35% in the blank control group to 22.8% in the 1 mg/ml group. Although the apoptosis of HepG2 cells was not concentration-dependent, it was significantly increased under the action of the drug concentration in this experiment and compared with the blank control group ($P < 0.001$). It can be seen that I-ATXP can effectively induce apoptosis of hepatoma cells HepG2, SMMC7721, and HKCI-C3, but there are differences in the degree of apoptosis.

The cell cycle is the basic process of cell life activities, including two consecutive methods: the division phase (M phase) and the intercellular phase. In the M phase, through mitosis, the intracellular double chromosomes separate and enter two different cells. In the intercellular phase, DNA replication is mainly car-

ried out. Intercellular phases include G0/G1 phase, S phase, and G2 phase. The G0/G1 phase is the preparation phase for DNA synthesis, the S phase is the DNA synthesis phase, and the G2 phase prepares the cell for mitosis. The division, proliferation, differentiation, and senescence of normal cells maintain the body's stability. Abnormal cell cycles can cause disorders in this process of cells, leading to the occurrence and development of tumors and other significant diseases [43]. Therefore, the study of tumor cell cycle regulation mechanism is significant for exploring tumor occurrence, development, clinical diagnosis, and treatment.

In order to further study whether I-ATXP also affects HepG2, SMMC7721 and HKCI-C3 cells through cell cycle inhibition, we used PI staining and flow cytometry to detect the cycle distribution of HepG2, SMMC7721, and HKCI-C3 cells after the drug was applied. The results show that different concentrations of I-ATXP increased the ratio of G0/G1 phase in the HepG2, SMMC7721 and HKCI-C3 cell cycle. In the interval of 0.125-1 mg/ml, the effect of I-ATXP was concentration-dependent. At the same time, I-ATXP can significantly reduce S-phase cell proportion in the three types of liver cancer cells. This result indicates that I-ATXP has a significant cycle inhibition effect on liver cancer cells HepG2, SMMC7721, and HKCI-C3, mainly inhibiting cells in the G0/G1 phase.

Our results also reflect that the apoptosis rate and cell G0/G1 phase ratio of the 5-Fu treatment group were significantly higher than those of the I-ATXP treatment groups, indicating that 5-Fu can induce three types of HepG2, SMMC7721, and HKCI-C3 HCC cells apoptosis and cycle arrest. The induction of apoptosis and cycle arrest was significantly more substantial than that of the I-ATXP group. In the cell proliferation experiment, the inhibitory effect of 5-Fu on the proliferation of the three liver cancer cells was also more significant than that of the I-ATXP group, indicating that 5-Fu can inhibit the growth and proliferation of liver cancer cells by inducing apoptosis and cycle arrest. The effect of -ATXP is similar to that of 5-Fu, suggesting that I-ATXP may also regulate the growth and proliferation of liver cancer cells through a similar mechanism. Still, the specific action details need to be further verified and analyzed.

Study on the effect of I-ATXP on the secretion of exosomes derived from HCC cells

After treating three different hepatocellular carcinoma cells with varying concentrations of I-ATXP (0.125-1 mg/ml) for 24 hours, we extracted the exosomes of the three hepatocarcinoma cells HepG2, SMMC7721, and HKCI-C3 with an exosome extraction kit. Using the acetylcholinesterase (AchE) experiment to detect the expression of exosomes, we discovered that different concentrations of I-ATXP can reduce the AchE value of liver cancer cells and the expression of liver cancer cell-specific proteins Alix and CD63 varies. As the drug concentration increases, there is a decreasing trend. Compared with the blank control group, in the high-dose group (1 mg/ml), the expressions of the exosomal-specific proteins, Alix and CD63, which were derived from the three hepatocarcinoma cells HepG2, SMMC7721, and HKCI-C3, were significantly decreased ($P < 0.0001$). The expression of CD63 varied in a classic-dose response fashion, whereas the decrease in Alix was seen only in the highest dosage.

Exosomes contain proteins, lipids, mRNAs, miRNAs, and other substances that reflect the source cells. These issues are also the direction and focus of our future experiments, which need to be further verified and confirmed on physiological and pathological statuses. The composition of exosomes from different sources may be different. Studies have shown that the level of tumor cell-derived exosomes is positively correlated with tumor cell proliferation, and tumor cell-derived exosomes play an essential role in tumor cell growth and proliferation regulation. Colon cancer cell exosomes contain the gene KRAS, which induces rapid cell growth through autocrine and paracrine pathways [46]. Gastric cancer cell exosomes activate P13K/Akt and MAPK/ERK signaling pathways through autocrine mechanisms to promote tumor cell proliferation [47]. In view of the fact that the contents of proteins and nucleic acids in exosomes can reflect the characteristics and status of the cells from which they originated, the changes in the physiology and pathology of exosomes must also be closely related to the changes in the status of

the cells from which they form. As a new mechanism of tumor regulation, the discovery and functional analysis of exosomes provide new directions and new ideas for tumor treatment. Traditional Chinese medicine is a potential treasure house of anticancer drugs. Research [48] confirmed a naphthoquinone substance extracted from comfrey, shikonin (Shikonin), with anti-tumor activity. It can inhibit the proliferation of human breast cancer cells by reducing tumor-derived exosomes and also provide a new way for the development of anti-tumor drugs. In this study, we preliminarily confirmed that I-ATXP could inhibit the secretion of exosomes derived from liver cancer cells and the protein expression of exosome-specific proteins, CD63 and Alix, when combined with the proliferation inhibition and apoptosis induction of I-AXTP. We question how to mediate or regulate exosomes and whether I-AXTP interacts with exosomes derived from liver cancer cells or if I-AXTP, as a traditional Chinese medicine compound, has similar functions like shikonin and is regulated by exosomes, tumor cells, and so on. These issues are also the direction and focus of our future experiments, which need to be further verified and confirmed.

Conclusions

Based on the above results, we come to the following conclusions: (*i*) I-ATXP has a significant inhibitory effect on the proliferation of hepatocarcinoma cells HepG2, SMMC7721, HKCI-C3, and is dependent on the time and concentration of the drug. Compared with the positive drug fluorouracil (5-Fu), Modified Aitongxiao Recipe is more selective and specific in inhibiting cell proliferation. This is also the advantage of traditional Chinese medicine in treating tumors and provides experimental evidence suggesting use for clinical treatment. (*ii*) I-ATXP can induce apoptosis and G0/G1 phase blockade of liver cancer cells. Combined with the results of cell proliferation experiments, I-ATXP can regulate the growth and proliferation of liver cancer cells by inducing apoptosis and cycle arrest of liver cancer cells. (*iii*) I-ATXP can inhibit the secretion of exosomes derived from liver cancer cells and the protein expression of exosomal-specific proteins CD63 and Alix, suggesting that I-ATXP may be secreted from liver cancer cells through exosomes which may be involved in the regulation of liver cancer cells. (*iv*) I-ATXP shows an ability to inhibit invasion of tissues by cancer cells. (*v*) exosomes derived from liver cancer cells can significantly promote the migration and invasion of homologous liver cancer cells.

Acknowledgements

We thank the following people for their contribution to this work. The Central Laboratory of Guangxi Medical University Xiao-Le Liang is acknowledged for his assistance with flow cytometry. Dara Brena is recognized for her assistance with edited references. The following grants supported this research: NIH/NIMHD 8G12MD007602; NIH/NIMHD 8U54MD007588; NSFC H2902.

Disclosure of conflict of interest

None.

Address correspondence to: Dr. Ming-Bo Huang, Department of Microbiology, Biochemistry and Immunology, Morehouse School of Medicine, 720 Westview, Drive, SW, Atlanta, Georgia 30310, USA. E-mail: mhuang@msm.edu; Dr. Jing Leng, Guangxi Key Laboratory of Translational Medicine for Treating High-Incidence Infectious Diseases with Integrative Medicine, Guangxi University of Chinese Medicine, Nanning 530200, Guangxi, China. E-mail: lengj@gxtcmu.edu.cn

References

[1] Siegel R, Naishadham D and Jemal A. Cancer statistics, 2013. CA Cancer J Clin 2013; 63: 11-30.

[2] Torre LA, Bray F, Siegel RL, Ferlay J, Lortet-Tieulent J and Jemal A. Global cancer statistics, 2012. CA Cancer J Clin 2015; 65: 87-108.

[3] Qu Z, Wu J, Wu J, Luo D, Jiang C and Ding Y. Exosomes derived from HCC cells induce sorafenib resistance in hepatocellular carcinoma both in vivo and in vitro. J Exp Clin Cancer Res 2016; 35: 159.

[4] Jemal A, Bray F, Center MM, Ferlay J, Ward E and Forman D. Global cancer statistics. CA Cancer J Clin 2011; 61: 69-90.

[5] Ferlay J, Shin HR, Bray F, Forman D, Mathers C and Parkin DM. Estimates of worldwide burden of cancer in 2008: GLOBOCAN 2008. Int J Cancer 2010; 127: 2893-2917.

[6] Zheng C, Zheng L, Yoo JK, Guo H, Zhang Y, Guo X, Kang B, Hu R, Huang JY, Zhang Q, Liu Z, Dong M, Hu X, Ouyang W, Peng J and Zhang Z. Landscape of infiltrating T cells in liver cancer

revealed by single-cell sequencing. Cell 2017; 169: 1342-1356, e1316.
[7] McGlynn KA and London WT. The global epidemiology of hepatocellular carcinoma: present and future. Clin Liver Dis 2011; 15: 223-243, vii-x.
[8] Grohmann M, Wiede F, Dodd GT, Gurzov EN, Ooi GJ, Butt T, Rasmiena AA, Kaur S, Gulati T, Goh PK, Treloar AE, Archer S, Brown WA, Muller M, Watt MJ, Ohara O, McLean CA and Tiganis T. Obesity drives STAT-1-dependent NASH and STAT-3-dependent HCC. Cell 2018; 175: 1289-1306, e1220.
[9] Kubo S, Takemura S, Sakata C, Urata Y and Uenishi T. Adjuvant therapy after curative resection for hepatocellular carcinoma associated with hepatitis virus. Liver Cancer 2013; 2: 40-46.
[10] Pai PC, Chuang CC, Tseng CK, Tsang NM, Chang KP, Yen TC, Liao CT, Hong JH and Chang JT. Impact of pretreatment body mass index on patients with head-and-neck cancer treated with radiation. Int J Radiat Oncol Biol Phys 2012; 83: e93-e100.
[11] Pu CY, Lan VM, Lan CF and Lang HC. The determinants of traditional Chinese medicine and acupuncture utilization for cancer patients with simultaneous conventional treatment. Eur J Cancer Care (Engl) 2008; 17: 340-349.
[12] Lin YH and Chiu JH. Use of Chinese medicine among patients with liver cancer in Taiwan. J Altern Complement Med 2010; 16: 527-528.
[13] Carmady B and Smith CA. Use of Chinese medicine by cancer patients: a review of surveys. Chin Med 2011; 6: 22.
[14] Wong LC, Chan E, Tay S, Lee KM and Back M. Complementary and alternative medicine practices among Asian radiotherapy patients. Asia Pac J Clin Oncol 2010; 6: 357-363.
[15] Thery C, Zitvogel L and Amigorena S. Exosomes: composition, biogenesis and function. Nat Rev Immunol 2002; 2: 569-579.
[16] Thery C, Amigorena S, Raposo G and Clayton A. Isolation and characterization of exosomes from cell culture supernatants and biological fluids. Curr Protoc Cell Biol 2006; Chapter 3: Unit 3.22.
[17] Chen R, Xu X, Tao Y, Qian Z and Yu Y. Exosomes in hepatocellular carcinoma: a new horizon. Cell Commun Signal 2019; 17: 1.
[18] Roma-Rodrigues C, Raposo LR, Cabral R, Paradinha F, Baptista PV and Fernandes AR. Tumor microenvironment modulation via gold nanoparticles targeting malicious exosomes: implications for cancer diagnostics and therapy. Int J Mol Sci 2017; 18: 162.
[19] Chen G, Huang AC, Zhang W, Zhang G, Wu M, Xu W, Yu Z, Yang J, Wang B, Sun H, Xia H, Man Q, Zhong W, Antelo LF, Wu B, Xiong X, Liu X, Guan L, Li T, Liu S, Yang R, Lu Y, Dong L, McGettigan S, Somasundaram R, Radhakrishnan R, Mills G, Lu Y, Kim J, Chen YH, Dong H, Zhao Y, Karakousis GC, Mitchell TC, Schuchter LM, Herlyn M, Wherry EJ, Xu X and Guo W. Exosomal PD-L1 contributes to immunosuppression and is associated with anti-PD-1 response. Nature 2018; 560: 382-386.
[20] Gougelet A. Exosomal microRNAs as a potential therapeutic strategy in hepatocellular carcinoma. World J Hepatol 2018; 10: 785-789.
[21] Milane L, Singh A, Mattheolabakis G, Suresh M and Amiji MM. Exosome mediated communication within the tumor microenvironment. J Control Release 2015; 219: 278-294.
[22] Yu DD, Wu Y, Shen HY, Lv MM, Chen WX, Zhang XH, Zhong SL, Tang JH and Zhao JH. Exosomes in development, metastasis and drug resistance of breast cancer. Cancer Sci 2015; 106: 959-964.
[23] Tang Y, Cui Y, Li Z, Jiao Z, Zhang Y, He Y, Chen G, Zhou Q, Wang W, Zhou X, Luo J and Zhang S. Radiation-induced miR-208a increases the proliferation and radioresistance by targeting p21 in human lung cancer cells. J Exp Clin Cancer Res 2016; 35: 7.
[24] Bobrie A, Colombo M, Krumeich S, Raposo G and Thery C. Diverse subpopulations of vesicles secreted by different intracellular mechanisms are present in exosome preparations obtained by differential ultracentrifugation. J Extracell Vesicles 2012; 1.
[25] Bobrie A and Thery C. Exosomes and communication between tumours and the immune system: are all exosomes equal? Biochem Soc Trans 2013; 41: 263-267.
[26] Luga V, Zhang L, Viloria-Petit AM, Ogunjimi AA, Inanlou MR, Chiu E, Buchanan M, Hosein AN, Basik M and Wrana JL. Exosomes mediate stromal mobilization of autocrine Wnt-PCP signaling in breast cancer cell migration. Cell 2012; 151: 1542-1556.
[27] Taylor DD and Gercel-Taylor C. Exosomes/microvesicles: mediators of cancer-associated immunosuppressive microenvironments. Semin Immunopathol 2011; 33: 441-454.
[28] Peinado H, Alecˇković M, Lavotshkin S, Matei I, Costa-Silva B, Moreno-Bueno G, Hergueta-Redondo M, Williams C, Garcia-Santos G, Ghajar CM, Nitadori-Hoshino A, Hoffman C, Badal K, Garcia BA, Callahan MK, Yuan J, Martins VR, Skog J, Kaplan RN, Brady MS, Wolchok JD, Chapman PB, Kang Y, Bromberg J and Lyden D. Corrigendum: melanoma exosomes educate bone marrow progenitor cells toward a pro-metastatic phenotype through MET. Nat Med 2016; 22: 1502.
[29] Peinado H, Aleckovic M, Lavotshkin S, Matei I, Costa-Silva B, Moreno-Bueno G, Hergueta-Re-

dondo M, Williams C, Garcia-Santos G, Ghajar C, Nitadori-Hoshino A, Hoffman C, Badal K, Garcia BA, Callahan MK, Yuan J, Martins VR, Skog J, Kaplan RN, Brady MS, Wolchok JD, Chapman PB, Kang Y, Bromberg J and Lyden D. Melanoma exosomes educate bone marrow progenitor cells toward a pro-metastatic phenotype through MET. Nat Med 2012; 18: 883-891.

[30] Soung YH, Nguyen T, Cao H, Lee J and Chung J. Emerging roles of exosomes in cancer invasion and metastasis. BMB Rep 2016; 49: 18-25.

[31] Riches A, Campbell E, Borger E and Powis S. Regulation of exosome release from mammary epithelial and breast cancer cells - a new regulatory pathway. Eur J Cancer 2014; 50: 1025-1034.

[32] Yang N, Li S, Li G, Zhang S, Tang X, Ni S, Jian X, Xu C, Zhu J and Lu M. The role of extracellular vesicles in mediating progression, metastasis and potential treatment of hepatocellular carcinoma. Oncotarget 2017; 8: 3683-3695.

[33] Yu LC, He CL and Chen CW. The role of exosomes in the pathogenesis, diagnosis and treatment of liver disease. Liver 2014; 211-214.

[34] Wei AL, Jian T, Chen YH, et al. Therapeutic effect analysis of Aitongxiao Granules in the treatment of primary liver cancer with blood stasis toxin and Zhengxiu syndrome. Liaoning Journal of Traditional Chinese Medicine 2007; 570-572.

[35] Gao LY, Wei AL, Pan Z, et al. Effect of Aitongxiao Granules on the expression of cytokine HIF-α mRNA and protein in hypoxic microenvironment of transplanted liver cancer model rats. Beijing Journal of Traditional Chinese Medicine 2014.

[36] Zhang YQ, Liu X and Wei AL. Effect of Aitongxiao Granules serum on proliferation and apoptosis of SMMC-7721 and Bel-7404 cells in vitro. Chinese Journal of Information on Traditional Chinese Medicine 2014; 21: 58-61.

[37] Wei AL, Wei LC and Tang J. The effect of Aitongxiao Granules on apoptosis in liver implanted walker-256 carcinosarcoma. Liaoning Journal of Traditional Chinese Medicine 2006; 515-516.

[38] Wei AL and Tang J. Experimental study on regulatory effect of Aitongxiao capsule on expression of VEGF in transplanted hepatocarcinoma 22 tumor of mice. Guangxi Journal of Traditional Chinese Medicine 2004; 27: 47-49.

[39] Wang Q, Wei AL and Xu Z. Experimental research on regulating the expression of VEGF, p53 and p21ras by Aitongxiao capsule. Guangxi Journal of Traditional Chinese Medicine 2005; 28: 45-48.

[40] Wei AL, Qiu ZJ and Lu HS. Intervention of Aitongxiao granule on VEGF-C in rat transplantation tumor model of liver cancer. Journal of Hubei University of Chinese Medicine 2010; 12: 14-16.

[41] Zhang Y, Wei A, Guo J, Tang J, Chen Y, Zhang X, Huang X and Liang L. Experimental research on apoptosis of rat transplanted hepatocellular carcinoma cell induced by Aitongxiao granule. Liaoning Journal of Traditional Chinese Medicine 2008; 35: 1091-1093.

[42] Jiang L, Tan AQ and Wei AL. Orthogonal experimental study on alcohol extraction technology of Aitongxiao granules. Lishizhen Medicine and Materia Medica Research 2009; 20: 1999-2000.

[43] Andre F, Schartz NE, Movassagh M, Flament C, Pautier P, Morice P, Pomel C, Lhomme C, Escudier B, Le Chevalier T, Tursz T, Amigorena S, Raposo G, Angevin E and Zitvogel L. Malignant effusions and immunogenic tumour-derived exosomes. Lancet 2002; 360: 295-305.

[44] Cai S, Luo B, Jiang P, Zhou X, Lan F, Yi Q and Wu Y. Immuno-modified superparamagnetic nanoparticles via host-guest interactions for high-purity capture and mild release of exosomes. Nanoscale 2018; 10: 14280-14289.

[45] Yamamoto KR, Alberts BM, Benzinger R, Lawhorne L and Treiber G. Rapid bacteriophage sedimentation in the presence of polyethylene glycol and its application to large-scale virus purification. Virology 1970; 40: 734-744.

[46] Weng Y, Sui Z, Shan Y, Hu Y, Chen Y, Zhang L and Zhang Y. Effective isolation of exosomes with polyethylene glycol from cell culture supernatant for in-depth proteome profiling. Analyst 2016; 141: 4640-4646.

[47] Kowal J, Arras G, Colombo M, Jouve M, Morath JP, Primdal-Bengtson B, Dingli F, Loew D, Tkach M and Thery C. Proteomic comparison defines novel markers to characterize heterogeneous populations of extracellular vesicle subtypes. Proc Natl Acad Sci U S A 2016; 113: E968-977.

[48] Greening DW, Xu R, Ji H, Tauro BJ and Simpson RJ. A protocol for exosome isolation and characterization: evaluation of ultracentrifugation, density-gradient separation, and immunoaffinity capture methods. Methods Mol Biol 2015; 1295: 179-209.

[49] Hong CS, Funk S, Muller L, Boyiadzis M and Whiteside TL. Isolation of biologically active and morphologically intact exosomes from plasma of patients with cancer. J Extracell Vesicles 2016; 5: 29289.

[50] Vickers KC, Palmisano BT, Shoucri BM, Shamburek RD and Remaley AT. MicroRNAs are transported in plasma and delivered to recipient cells by high-density lipoproteins. Nat Cell Biol 2011; 13: 423-433.

[51] Boing AN, van der Pol E, Grootemaat AE, Coumans FA, Sturk A and Nieuwland R. Single-step

isolation of extracellular vesicles by size-exclusion chromatography. J Extracell Vesicles 2014; 3.
[52] Huang MB, Gonzalez RR, Lillard J and Bond VC. Secretion modification region-derived peptide blocks exosome release and mediates cell cycle arrest in breast cancer cells. Oncotarget 2017; 8: 11302-11315.
[53] Huang F and Wei AL. The effect on miRNAs of replant liver cancer rats treated by Aitongxiao granule. Chin Pharm J 2013; 48: 1740-1743.
[54] Sung H, Ferlay J, Siegel RL, Laversanne M, Soerjomataram I, Jemal A and Bray F. Global cancer statistics 2020: GLOBOCAN estimates of incidence and mortality worldwide for 36 cancers in 185 countries. CA Cancer J Clin 2021; 71: 209-249.
[55] Hatanaka T, Naganuma A and Kakizaki S. Lenvatinib for hepatocellular carcinoma: a literature review. Pharmaceuticals (Basel) 2021; 14: 36.